Global Change Biology (2006) **12,** 710–730, doi: 10.1111/j.1365-2486.2006.01121.x

# Combining meteorology, eddy fluxes, isotope measurements, and modeling to understand environmental controls of carbon isotope discrimination at the canopy scale

J. N. ARANIBAR*†, J. A. BERRY†, W. J. RILEY‡, D. E. PATAKI§, B. E. LAW¶ and J. R. EHLERINGER*

*Department of Biology, University of Utah, Salt Lake City, UT, USA, †Department of Global Ecology, Carnegie Institution of Washington, Stanford, CA, USA, ‡Lawrence Berkeley National Laboratory, Earth Sciences Division, Berkeley, CA, USA, §Department of Earth System Sciences, Department of Ecology and Evolutionary Biology, University of California, Irvine, Irvine, CA, USA, ¶College of Forestry, Oregon State University, Corvallis, OR, USA

**Abstract**

**Estimates of terrestrial carbon isotope discrimination are useful to quantify the terrestrial carbon sink. Carbon isotope discrimination by terrestrial ecosystems may vary on seasonal and interannual time frames, because it is affected by processes (e.g. photosynthesis, stomatal conductance, and respiration) that respond to variable environmental conditions (e.g. air humidity, temperature, light). In this study, we report simulations of the temporal variability of canopy-scale $C_3$ photosynthetic carbon isotope discrimination obtained with an ecophysiologically based model (ISOLSM) designed for inclusion in global models. ISOLSM was driven by half-hourly meteorology, and parameterized with eddy covariance measurements of carbon and energy fluxes and foliar carbon isotope ratios from a pine forest in Metolius (OR). Comparing simulated carbon and energy fluxes with observations provided a range of parameter values that optimized the simulated fluxes. We found that the sensitivity of photosynthetic carbon isotope discrimination to the slope of the stomatal conductance equation (*m*, Ball–Berry constant) provided an additional constraint to the model, reducing the wide parameter space obtained from the fluxes alone. We selected values of *m* that resulted in similar simulated long-term discrimination as foliar isotope ratios measured at the site. The model was tested with $^{13}C$ measurements of ecosystem ($\delta_R$) and foliar ($\delta_f$) respiration. The daily variability of simulated $^{13}C$ values of assimilated carbon ($\delta_A$) was similar to that of observed $\delta_f$, and higher than that of observed and simulated $\delta_R$. We also found similar relationships between environmental factors (i.e. vapor pressure deficit) and simulated $\delta_R$ as measured in ecosystem surveys of $\delta_R$. Therefore, ISOLSM reasonably simulated the short-term variability of $\delta_A$ controlled by atmospheric conditions at the canopy scale, which can be useful to estimate the variability of terrestrial isotope discrimination. Our study also shows that including the capacity to simulate carbon isotope discrimination, together with simple ecosystem isotope measurements, can provide a useful constraint to land surface and carbon balance models.**

*Keywords:* atmospheric controls, biosphere–atmosphere exchange, canopy scale, carbon fluxes, carbon isotope discrimination, ecophysiological model, eddy fluxes, parameter constraints, photosynthesis, stomatal conductance

*Received 9 March 2005; revised version received 19 October 2005; accepted 25 October 2005*

Correspondence: J. N. Aranibar, Department of Biology, University of Utah, Salt Lake City, UT, USA, fax + 650 462 5968, e-mail: aranibar@alumni.virginia.edu

## Introduction

The carbon isotope ratio of atmospheric $CO_2$ is an important measurement used to quantify ocean and terrestrial exchange processes in the global carbon balance (Ciais *et al*., 1995, 2005; Fung *et al*., 1997). $^{13}C$ is particularly useful because discrimination by oceanic uptake is about 10 times lower than that by $C_3$ photosynthetic uptake. Carbon isotope ratios are also widely used in ecological research as tracers and nondestructive integrators of how organisms interact with, and respond to, their abiotic and biotic environments (Dawson *et al*., 2002). Carbon isotopes have the potential, therefore, to facilitate an integration of ecology and geology with the current interest in carbon cycle processes. However, these links have been difficult to make, in part because of a lack of quantitative tools needed to integrate isotopic processing across temporal and spatial scales.

Toward this end, there is now an effort to construct isotope fractionation earth system models (Cuntz *et al*., 2003; Hoffmann *et al*., 2004). The atmospheric sampling networks (i.e. CSIRO, Francey *et al*., 1995; NOAA, Trolier *et al*., 1996) and the ice core programs provide important data that define the isotopic composition of the global atmosphere and how it has changed over the past several hundred thousand years (Hammer *et al*., 1997; Indermühle *et al*., 1999; Trudinger *et al*., 1999). These measurements constrain the total mass and isotope balance of exchanges between the atmosphere, oceans, and terrestrial biosphere, and models must match these constraints. However, the discrimination by terrestrial ecosystems is not geographically uniform and may vary on seasonal and interannual time frames. Imperfect knowledge of these variations is a significant uncertainty in applying isotopic constraints to the global carbon cycle (Kaplan *et al*., 2002; Randerson *et al*., 2002; Scholze *et al*., 2003), and a challenge for earth system models. Terrestrial ecosystem discrimination may vary by photosynthetic type ($C_3$ or $C_4$) and, at least for $C_3$ plants, in response to a wide range of environmental factors and stresses (Lloyd & Farquhar, 1994; Randerson *et al*., 2002; Miller *et al*., 2003). These uncertainties imply a need for isotope fractionating ecosystem models suitable for integration into earth system models and for a corresponding framework of ecosystem measurements for model calibration and testing.

Terrestrial $CO_2$ exchange between the biosphere and the atmosphere is controlled by photosynthetic carbon uptake and respiration. There is a solid theoretical understanding of photosynthesis and its associated discrimination at the leaf scale. The Farquhar *et al*. (1980) photosynthesis model and semi-mechanistic models of stomatal conductance (Ball, 1988; Leuning *et al*., 1998) have been included in models to simulate carbon and water exchange in different sites and environmental conditions (CANVEG, Baldocchi, 1997; LSM, Bonan, 1996; ACASA, Pyles *et al*., 2000; SiB2, Sellers *et al*., 1996). A theoretical treatment of carbon isotope discrimination in $C_3$ photosynthesis (Farquhar *et al*., 1982) has been incorporated into some of these models to permit calculations of $^{13}C$ discrimination (CANISOTOPE, Baldocchi & Bowling, 2003; SiB2, Suits *et al*., 2005). Global simulations of $^{13}C$ discrimination have been run at different spatial and temporal scales, driven by long-term average meteorology (Buchmann & Kaplan, 2001; Kaplan *et al*., 2002; Scholze *et al*., 2003), global circulation models (Fung *et al*., 1997), meteorology from reanalysis products, and remote sensing data (Still *et al*., 2003; Suits *et al*., 2005). Canopy scale models have also been adapted for simulations of within canopy gradients in the isotopic composition of $CO_2$, to evaluate $\delta^{13}C$ sampling strategies, and the partitioning of net ecosystem carbon exchange (*NEE*, $\mu mol\, m^{-2}\, s^{-1}$) into photosynthesis and respiration (Ogee *et al*., 2003, 2004; Baldocchi & Bowling, 2005). However, these models are significantly more complex than the models that simulate only the mass fluxes, and it is still not clear whether the models and the isotopic measurements required to test them add significant value to the flux measurements.

The growing availability of isotopic, meteorological, and eddy flux data through international networks (i.e. AmeriFlux, FLUXNET, Law *et al*., 2002, CarboEurope, http://www.carboeurope.org, and BASIN, http://basinisotopes.org) provides an opportunity to rigorously evaluate models of biosphere–atmosphere carbon exchange. At the site level, *NEE* fluxes are being measured using eddy-covariance at many sites around the world (Baldocchi *et al*., 2001). Interpreting these measurements is complicated as they are a composite of respired and assimilated fluxes. Further, the respired $CO_2$ flux is a combination of autotrophic respiration from roots, stems, and foliage and heterotrophic respiration from soil and detritus. All of these processes occur in an open system with strong turbulent mixing. Several approaches have been taken to obtain isotopic information about these exchange processes with the intention to partition the *NEE* fluxes into photosynthesis and respiration and to estimate terrestrial ecosystem discrimination. These include estimating the isotope composition of *NEE*, fixed carbon pools, and the $CO_2$ produced in respiration by the ecosystem. Measurements of covariation of $CO_2$ concentration and isotopic ratios in the air above or within canopies can be used to estimate short-term variation in the isotope ratios of *NEE* (Bowling *et al*., 2001b; Lai *et al*., 2004), but this is a

very difficult measurement and it is not generally available at eddy covariance sites.

Measurements of the $\delta^{13}C$ value of plant tissue, which are commonly available at numerous sites around the world (Pataki *et al.*, 2003; Hemming *et al.*, 2005), integrate all the processes and interactions that effect growth and carbon balance over the time that the carbon accumulates. This metric provides a good constraint on net carbon gain but very limited insight into individual processes or their variation in time. $\delta^{13}C$ values of leaf and phloem sugars reflect the variability of canopy photosynthesis and conductance but they are affected by temporal lags between carbon fixation and phloem transport, and mixing of carbon assimilated at different times (Keitel *et al.*, 2003; Scartazza *et al.*, 2004; Barbour *et al.*, 2005). Nevertheless, these isotopic measurements place constraints on a model of isotopic discrimination in photosynthesis and respiration.

An alternative approach to estimate the variability of ecosystem discrimination is to sample the $CO_2$ produced in respiration by the ecosystem. If respiration is in steady state with photosynthesis and there is no other major pathway of carbon export from the ecosystem, then the isotopic composition of respired $CO_2$ should equal that of assimilated carbon. Isotope ratios of soil, foliar, and ecosystem respired $CO_2$ are assumed to reflect those of the substrate for respiration, either soil organic or plant carbon and ultimately, the photosynthetic inputs, because discrimination against $^{13}C$ during respiration is generally assumed to be negligible (Lin & Ehleringer, 1997; but see Ghashghaie *et al.*, 2001 and Ghashghaie *et al.*, 2003). The isotopic composition of integrated ecosystem respiration ($\delta_R$, ‰) can be obtained from measurements of the concentration and isotope ratios of $CO_2$ in night-time ambient air with the Keeling plot method (Keeling, 1958; Pataki *et al.*, 2003) and that of component processes by chamber measurements (McDowell *et al.*, 2004a). A promising adaptation of this approach comes from studies that have demonstrated that a significant proportion of soil $CO_2$ efflux from ecosystems derives from recent assimilates. This was first demonstrated in girdling studies (Ekblad & Högberg, 2001; Högberg *et al.*, 2001) that showed an approximately 50% reduction in soil $CO_2$ release when translocation of recent photosynthates from the leaves to the roots was interrupted. Other studies have shown that variation in the isotopic composition of $CO_2$ respired by some ecosystems (using Keeling plot analysis) vary in synchrony with synoptic weather cycles (Bowling *et al.*, 2002; Ometto *et al.*, 2002; Knohl *et al.*, 2005; Mortazavi *et al.*, 2005). McDowell *et al.* (2004a) showed that the isotope composition of leaf respiration ($\delta_f$, ‰) also appeared to vary with weather conditions that should effect carbon isotope discrimination.

The results of these isotopic studies have been qualitatively consistent with what would be expected based on our theoretical understanding of the discrimination process and known responses of photosynthesis and stomatal conductance to environmental conditions. However, the quantitative basis for these observations has not been investigated, and modeling provides one approach to do this. The present work reports on simulations of carbon isotope fractionation in photosynthesis in a land surface model designed for inclusion in global models (LSM, Bonan, 1996; ISOLSM, Riley *et al.*, 2002). ISOLSM was driven by meteorological data from a semi-arid pine forest (Metolius, OR) and the model results were compared with eddy covariance and isotope measurements made at the site. Parameter values used in the model were adjusted to obtain agreement between simulated and measured carbon and energy fluxes, and $\delta^{13}C$ values of foliage. The simulations were tested against daily observations of $\delta_f$ and $\delta_R$ made at the site during a period of variable environmental conditions.

## Methods

### *Study site*

We ran and tested ISOLSM using 2000–2001 meteorological, isotopic, and eddy covariance measurements from a relatively undisturbed old-growth ponderosa pine forest in central Oregon. This site is part of the AmeriFlux network, and is located in the Metolius Research Natural Area (44° 30′ N, 121° 37′ W, elevation 915 m). The site has never been logged and consists of old ( ~ 250 years), young ( ~ 45 years), and mixed patches of ponderosa pines. The canopy is relatively open with a maximum height of about 43 m. The understory vegetation is sparse, and the estimated rooting depth is 1.5 m, although some roots may reach up to 5 m depth (Williams *et al.*, 2001). A significant proportion of the water used by the vegetation (up to 47%) is thought to be extracted from below 80 cm depth, so this old forest appears to be buffered from the effect of seasonal droughts (Irvine *et al.*, 2004; Schwarz *et al.*, 2004). The site has warm dry summers and cool wet winters. Precipitation varies between 300 and 600 mm $yr^{-1}$, mostly occurring between October and June, with the summer months mostly lacking precipitation (Law *et al.*, 2001b; Irvine *et al.*, 2004). Summer precipitation during 2000 was 9.8 mm; other climate characteristics during that year are described in Anthoni *et al.* (2002). Site characteristics used in the model are detailed in Table 2.

**Table 1** Symbols used in the text

| | |
|---|---|
| $A$ | = gross photosynthesis ($\mu mol\, m^{-2}\, s^{-1}$) |
| $a$ | = carbon isotope fractionation during diffusion across the stomatal cavity, 4.4‰ |
| $ab$ | = carbon isotope fractionation during diffusion across the boundary layer, 2.9‰ |
| $as$ | = carbon isotope fractionation during diffusion in water, 0.7‰ |
| $BIAS$ | = slope of a linear regression line of simulated vs. observed $H$, $LE$, and $NEE$ data pairs (dimensionless) |
| $b$ | = carbon isotope fractionation by Rubisco $CO_2$ fixation, assuming 5% of PEP fixation, 28.2‰ |
| $b_p$ | = minimum stomatal conductance when $A = 0$ ($\mu mol\, m^{-2}\, s^{-1}$) |
| $C$ | = adjustment factor for energy balance closure (dimensionless) |
| $^{13}C_a$ | = isotope ratio of atmospheric $CO_2$ (dimensionless) |
| $^{13}C_p$ | = isotope ratio of assimilated carbon (dimensionless) |
| $c_a$ | = $CO_2$ concentration in ambient air ($mol\, mol^{-1}$) |
| $c_c$ | = $CO_2$ concentration at sites of carboxylation ($mol\, mol^{-1}$) |
| $c_i$ | = $CO_2$ concentration in the stomatal cavity ($mol\, mol^{-1}$) |
| $c_s$ | = $CO_2$ concentration at the leaf surface, ($mol\, mol^{-1}$) |
| $ees$ | = carbon isotope fractionation as $CO_2$ enters solution, 1.1‰ |
| $^{13}F_A$ | = gross $^{13}C$ fluxes from the atmosphere to the leaf ($\mu mol\, m^{-2}\, s^{-1}$) |
| $^{12}F_A$ | = gross $^{12}C$ fluxes from the atmosphere to the leaf ($\mu mol\, m^{-2}\, s^{-1}$) |
| $G$ | = soil heat flux ($W\, m^{-2}$) |
| $G_c$ | = canopy conductance ($\mu mol\, m^{-2}\, s^{-1}$) |
| $g_s$ | = stomatal conductance ($\mu mol\, m^{-2}\, s^{-1}$) |
| $g_w$ | = mesophyll wall conductance ($\mu mol\, m^{-2}\, s^{-1}$) |
| $H$ | = sensible heat flux ($W\, m^{-2}$) |
| $K_c$ | = Michaelis–Menten constant for $CO_2$ (Pa) |
| $K_o$ | = Michaelis–Menten constant for $O_2$ (Pa) |
| $LE$ | = latent heat flux ($W\, m^{-2}$) |
| $m$ | = Ball–Berry constant (dimensionless) |
| $NEE$ | = net ecosystem exchange of $CO_2$, positive during uptake ($\mu mol\, m^{-2}\, s^{-1}$) |
| $NSEE$ | = normalized standard error of the estimate (dimensionless) |
| $o_i$ | = $O_2$ partial pressure (Pa) |
| $p$ | = atmospheric pressure (Pa) |
| $p_c$ | = $CO_2$ partial pressure at sites of carboxylation (Pa) |
| $q$ | = quantum efficiency ($\mu mol\, CO_2\, \mu mol^{-1}$ photon) |
| $R$ | = relative humidity (dimensionless) |
| $r_b$ | = leaf boundary layer resistance ($s\, m^2\, \mu mol^{-1}$) |
| $R_f$ | = foliar respiration rate ($\mu mol\, m^{-2}\, s^{-1}$) |
| $R_m$ | = microbial respiration rate ($\mu mol\, m^{-2}\, s^{-1}$) |
| $R_n$ | = net radiation ($W\, m^{-2}$) |
| $R_{PDB}$ | = carbon isotope ratio of standard PDB (dimensionless) |
| $R_r$ | = root respiration rate ($\mu mol\, m^{-2}\, s^{-1}$) |
| $R_s$ | = stem respiration rate ($\mu mol\, m^{-2}\, s^{-1}$) |
| $r_s$ | = stomatal resistance ($s\, m^2\, \mu mol^{-1}$) |
| $V_m$ | = maximum carboxylation rate at 25 °C ($\mu mol\, m^{-2}\, s^{-1}$) |
| $VPD$ | = vapor pressure deficit (kPa) |
| $W_c$ | = Rubisco-limited rate of carboxylation ($\mu mol\, m^{-2}\, s^{-1}$) |
| $W_e$ | = export-limited rate of carboxylation ($\mu mol\, m^{-2}\, s^{-1}$) |
| $W_j$ | = light-limited rate of carboxylation ($\mu mol\, m^{-2}\, s^{-1}$) |
| $\alpha$ | = fractionation factor of photosynthesis (dimensionless) |
| $\phi$ | = absorbed photosynthetically active radiation ($W\, m^{-2}$) |
| $\Gamma_*$ | = $CO_2$ compensation point (Pa) |
| $\delta^{13}C$ | = carbon isotope composition of $CO_2$relative to a standard (PDB) (‰) |
| $\delta_A$ | = $\delta^{13}C$ of assimilated carbon (‰) |
| $\delta_f$ | = $\delta^{13}C$ of foliar respiration (‰) |
| $\delta_m$ | = $\delta^{13}C$ of microbial respiration (‰) |
| $\delta_R$ | = $\delta^{13}C$ of ecosystem respiration (‰) |
| $\delta_r$ | = $\delta^{13}C$ of root respiration (‰) |
| $\delta_s$ | = $\delta^{13}C$ of stem respiration (‰) |
| $\overline{\delta_A}$ | = flux-weighted annual averaged $\delta^{13}C$ of assimilated carbon (‰) |
| $\Delta$ | = discrimination by photosynthesis (‰) |

### *Model description*

ISOLSM is based on the land surface model LSM1 (Bonan, 1996), which was modified to simulate oxygen and carbon isotope discrimination (Riley *et al*., 2002, 2003). The model simulates energy, water, and carbon fluxes among the soil, canopy, and atmosphere at a user-defined time step (here 10 min), using half-hourly measured meteorological inputs (Table 2). We assumed that soil water did not limit stomatal conductance or photosynthesis because modeling, sapflow, and isotopic studies suggest that the deep rooted trees of this site have permanent access to water (Law *et al*., 2001b; Williams *et al*., 2001; Bowling *et al*., 2003; Irvine *et al*., 2004; Schwarz *et al*., 2004).

The canopy is represented as a single layer, but is partitioned into sunlit and shaded fractions, with different photosynthetic rates that depend on the amount of absorbed photosynthetically active radiation ($\phi$, $W\, m^{-2}$). Canopy conductance ($G_c$, $\mu mol\, m^{-2}\, s^{-1}$) is integrated considering the sunlit and shaded leaf area indices, and the photosynthesis and stomatal conductance calculated for each canopy fraction (Bonan, 1996). Photosynthesis and stomatal conductance are simulated iteratively using the parameterizations of Farquhar *et al*. (1980) and Collatz *et al*. (1991). However, in the current version of the model the photosynthesis calculation was modified to include the diffusion of $CO_2$ from the

**Table 2** Site characteristics and data used as model inputs and to compare to model outputs

| | Dimension | Value/data type | Source |
|---|---|---|---|
| Input data | | | |
| Vegetation type | — | Temperate coniferous forest | Law *et al*. (2001b) |
| Canopy height | m | 34 | Law *et al*. (2001b) |
| Leaf area index | — | 2 | Law *et al*. (2003) |
| Soil carbon to 1 m depth | $kg\,m^{-2}$ | 5.87 | Law *et al*. (2001b) |
| Root biomass to 1 m depth | $kg\,m^{-2}$ | 3.99 | Law *et al*. (2003) |
| Soil texture: sand, silt, clay | % | 65, 25, 10 | Law *et al*. (2001b) |
| $\delta^{13}C$ of soil organic matter | ‰ | −26.2 | BASIN, Bowling *et al*. (2002) |
| Air temperature | °C | Half-hourly data | AmeriFlux |
| Wind speed | $m\,s^{-1}$ | Half-hourly data | AmeriFlux |
| Incoming solar radiation | $W\,m^{-2}$ | Half-hourly data | AmeriFlux |
| Relative humidity | — | Half-hourly data | AmeriFlux |
| Vapor pressure deficit | kPa | Half-hourly data | |
| Precipitation | mm | Half-hourly data | AmeriFlux |
| Data compared with model outputs | | | |
| Net radiation | $W\,m^{-2}$ | Half-hourly data | AmeriFlux |
| Latent heat | $W\,m^{-2}$ | Half-hourly eddy flux data | AmeriFlux |
| Sensible heat | $W\,m^{-2}$ | Half-hourly eddy flux data | AmeriFlux |
| Net ecosystem carbon exchange | $\mu mol\,m^{-2}\,s^{-1}$ | Half-hourly eddy flux data | AmeriFlux |
| $\delta^{13}C$ of old leaves | ‰ | −26.9 | BASIN |
| $\delta^{13}C$ of ecosystem respiration | ‰ | Night-time Keeling plot estimates | BASIN, Bowling *et al*. (2002), McDowell *et al*. (2004a) |

stomatal cavity to the chloroplast. Leaf photosynthetic uptake is taken as the minimum of three potential uptake rates with separate limitations:

Rubisco-limited rate of carboxylation ($W_c$, $\mu mol\,m^{-2}\,s^{-1}$)

$$W_c = \frac{(p_c - \Gamma_*)V_m}{p_c + K_c(1 + o_i/K_o)}. \quad (1)$$

Light-limited rate of carboxylation ($W_j$, $\mu mol\,m^{-2}\,s^{-1}$)

$$W_j = \frac{(p_c - \Gamma_*)4.6\phi q}{p_c + 2\Gamma_*}. \quad (2)$$

Export-limited rate of carboxylation ($W_e$, $\mu mol\,m^{-2}\,s^{-1}$)

$$W_e = 0.5V_m. \quad (3)$$

Where $p_c$ is the partial pressure of $CO_2$ in the sites of carboxylation (Pa), $V_m$ the maximum rate of carboxylation at 25 °C ($\mu mol\,m^{-2}\,s^{-1}$), $o_i$ the partial pressure of $O_2$ (Pa), $K_c$ and $K_o$ are the Michaelis–Menten constants for $CO_2$ and $O_2$ (Pa), $\Gamma_*$ the compensation point (Pa), and $q$ the quantum efficiency ($\mu mol\,CO_2\,\mu mol^{-1}$ photon). Note that $p_c$ is in units of partial pressure, and is given by $p_c = c_c p$, where $p$ is atmospheric pressure (Pa) and $c_c$ is the $CO_2$ concentration at sites of carboxylation expressed in mole fraction (i.e. $mol\,mol^{-1}$). Biochemical constants associated with the kinetic properties of Rubisco, such as $K_c$, $K_o$, and $\Gamma_*$, are generally conserved for most higher terrestrial plants with $C_3$ photosynthesis (von Caemmerer, 2000). The default parameters of LSM ($K_c = 30$ Pa and $K_o = 30\,000$ Pa) were changed to $K_c = 32$ Pa and $K_o = 17\,900$ Pa. The new set give better agreement of simulated $\Gamma_*$, $CO_2$ concentration in the stomatal cavity ($c_i$, $mol\,mol^{-1}$), and discrimination to observations (von Caemmerer *et al*., 1994; von Caemmerer, 2000; Bernacchi *et al*., 2001). However, the correct set of these constants is still open to debate.

Stomatal conductance ($g_s$, $\mu mol\,m^{-2}\,s^{-1}$) and $CO_2$ concentration at the sites of carboxylation are calculated iteratively with photosynthesis

$$c_c = c_s - A(1.65r_s + 1/g_w), \quad (4)$$

where $c_s$ is the $CO_2$ concentration at the leaf surface ($mol\,mol^{-1}$), $A$ the gross photosynthesis ($\mu mol\,m^{-2}\,s^{-1}$), $r_s$ the stomatal resistance to water vapor ($s\,m^2\,\mu mol^{-1}$) and is equal to $1/g_s$, 1.65 the ratio of the molecular diffusivities of $H_2O$ to $CO_2$, and $g_w$ mesophyll wall conductance to $CO_2$ ($\mu mol\,m^{-2}\,s^{-1}$)

$$g_w = 4800V_m. \quad (5)$$

Following Evans and von Caemmerer (1996) we assume this conductance is proportional to the Rubisco content. The constant 4800, which is comparable to those reported by Evans and Loreto (2000), was chosen to obtain $^{13}C$ discrimination consistent with field observations and a drawdown of $CO_2$ partial pressure from

stomatal cavity to the chloroplasts at high photosynthetic rates of about 3–3.5 Pa. However, simulations with different values of this constant were performed, in order to analyze the sensitivity of discrimination, carbon and energy fluxes to this parameter.

Stomatal conductance is calculated with the Ball–Berry equation (Ball, 1988)

$$\frac{1}{r_s} = m\frac{A}{c_s}R + b_p, \tag{6}$$

where $m$ is the Ball–Berry constant (dimensionless) (Ball, 1988), $R$ the relative humidity (dimensionless), and $b_p$ the minimum stomatal conductance ($\mu mol\, m^{-2}\, s^{-1}$) when $A = 0$. The $CO_2$ concentration at the leaf surface is calculated as

$$c_s = c_a - 1.37 r_b A, \tag{7}$$

where $c_a$ is the $CO_2$ concentration in the atmosphere ($mol\, mol^{-1}$) and $r_b$ the boundary layer resistance ($s\, m^2\, \mu mol^{-1}$). The value 1.37 accounts for the difference in leaf boundary layer diffusivity between $H_2O$ and $CO_2$. Then, the $CO_2$ concentration in the stomata is calculated as

$$c_i = c_s - 1.65 r_s A, \tag{8}$$

where the value 1.65 accounts for the difference in molecular diffusivities of $H_2O$ and $CO_2$.

The isotopic discrimination caused by photosynthesis ($\Delta$, ‰) is defined as

$$\Delta = (\alpha - 1)1000, \tag{9}$$

where $\alpha$, the fractionation factor, is

$$\alpha = {}^{13}C_a / {}^{13}C_p \tag{10}$$

and $^{13}C_a$ and $^{13}C_p$ are the isotope ratios of the heavy to the light isotope (dimensionless) in atmospheric $CO_2$ and assimilated carbon, respectively. Atmospheric $CO_2$ was assumed to have a constant isotope ratio during the whole year (0.0111495), equal to −7.8‰ in the delta notation.

We calculated $\Delta$ including the fractionation occuring during diffusion of $CO_2$ from the atmosphere to the sites of carboxylation, and by fixation of $CO_2$ in the chloroplasts (Farquhar *et al*., 1989)

$$\Delta = \frac{(ab(c_a - c_s)) + (a(c_s - c_i) + (ees + as)(c_i - c_c) + bc_c}{c_a}, \tag{11}$$

where $ab = 2.9$‰, fractionation during the diffusion across the boundary layer (Farquhar, 1983); $a = 4.4$‰, fractionation during the diffusion across stomatal cavity (Craig, 1954); $ees = 1.1$‰, fractionation occurring as $CO_2$ enters solution (O'Leary, 1984); $as = 0.7$‰, fractionation due to diffusion in water (O'Leary, 1984); and $b = 28.2$‰, fractionation by Rubisco $CO_2$ fixation, assuming 5% PEP (phosphoenolpyruvate) fixation (Farquhar, 1983; Suits *et al*., 2005).

The gross leaf $^{13}CO_2$ and $^{12}CO_2$ fluxes, $^{13}F_A$ and $^{12}F_A$ ($\mu mol\, m^{-2}\, s^{-1}$), respectively, were calculated as

$${}^{13}F_A = \frac{A\,{}^{13}C_a}{\alpha + {}^{13}C_a}, \tag{12}$$

$${}^{12}F_A = A - {}^{13}F_A, \tag{13}$$

where $\alpha$, the fractionation factor, is derived from Eqn (9).

Finally, the $\delta^{13}C$ value of assimilated carbon ($\delta_A$, ‰) was calculated as

$$\delta_A = \left(\frac{{}^{13}F_A/{}^{12}F_A}{R_{pdb}} - 1\right)1000, \tag{14}$$

where $R_{pdb}$ (0.0112372) is the isotope ratio of the standard for $^{13}C$, Pee Dee Belemnite (Hoefs, 1997).

### *Soil respiration and* $\delta_R$

Soil respiration is partitioned in the model into root ($R_r$, $\mu mol\, m^{-2}\, s^{-1}$) and microbial ($R_m$, $\mu mol\, m^{-2}\, s^{-1}$) respiration. Both are temperature dependent, and microbial respiration is also affected by soil moisture. Other respiratory fluxes include stem ($R_s$, $\mu mol\, m^{-2}\, s^{-1}$) and foliar ($R_f$, $\mu mol\, m^{-2}\, s^{-1}$) respiration, both of which are temperature dependent (Bonan, 1996). Using reported values of root biomass (fine and coarse) and soil carbon to 1 m depth (Table 2), model simulations indicated that about half of soil respiration derived from root respiration and half from microbial respiration. This partitioning is close to previous estimates for this site, which attribute 43%, 53%, and 42% of respiration to heterotrophic sources in spring, summer, and autumn, respectively (Law *et al*., 2001b). The calculations of $\delta^{13}C$ values of respiratory components do not take into account possible fractionation effects during respiration, because different respiratory processes may result in higher and lower values of $\delta^{13}C$ of the respired $CO_2$ (Ghashghaie *et al*., 2003; Klumpp *et al*., 2005). It is not clear how these processes would affect the total respired $CO_2$ in uncontrolled ecosystem conditions. In this study, $\delta_f$ was set equal to $\delta_A$, and the $\delta^{13}C$ value of microbial respiration ($\delta_m$, ‰) was assumed to be constant and equal to that of the measured soil organic matter, including litter (−26.2‰, Table 2). $\delta^{13}C$ values of root ($\delta_r$, ‰) and stem ($\delta_s$, ‰) respiration were assumed to be the same as recently assimilated carbon. We did not attempt to represent time lags in the transport of assimilates to different plant pools, and we assumed an arbitrary time lag of 1 day between assimilation and root and stem respiration. A larger delay in the coupling between root respiration and assimilation would cause

a phase shift and slightly attenuate the temporal variation in $\delta_R$.

Finally, the simulated night-time integral of $\delta_R$ was calculated as

$$\delta_R = \sum_{i=1}^{n} \left( \frac{\delta_{mi} R_{mi} + \delta_{ri} R_{ri} + \delta_{fi} R_{fi} + \delta_{si} R_{si}}{R_{mi} + R_{ri} + R_{fi} + R_{si}} \right), \quad (15)$$

where $n$ is the number of half-hourly simulation outputs from dusk to dawn for each night.

### *Data used to drive and test the model*

Carbon dioxide, water vapor, and energy fluxes used to parameterize the model were estimated half-hourly in 2000 using the eddy covariance technique (Law *et al*., 2001b). Details on the instrumentation, flux correction methods, and calculations are reported in Anthoni *et al*. (2002). Meteorological variables used to drive the model, including air temperature, vapor pressure deficit (*VPD*, Pa), incoming solar radiation, net radiation, and rainfall were also measured half-hourly at the top of the flux towers in 2000 and 2001 (Table 2). The flux and climate data are available from the AmeriFlux network (http://public.ornl.gov/ameriflux/).

Organic material from soils and foliage, and $CO_2$ of canopy air were analyzed for $\delta^{13}C$ (Bowling *et al*., 2002) and these isotopic data are available from the BASIN network (http://basinisotopes.org/). $\delta_R$ was estimated in Metolius in 2000 and 2001 using the Keeling plot approach (Bowling *et al*., 2002; McDowell *et al*., 2004a). Nocturnal air samples were collected, chemically dried with magnesium perchlorate, and analyzed for $CO_2$ concentration with an IRGA according to Bowling *et al*. (2001a), and for $\delta^{13}C$ by continuous flow IRMS as in Ehleringer and Cook (1998). During selected days of 2001, McDowell *et al*. (2004a) also estimated the isotopic ratios of foliage respiration representative of old trees located in sunlit portions of the canopy. $\delta_R$ and $\delta_f$ were estimated as the intercept of a geometric mean regression of $1/CO_2$ and $\delta^{13}C$ (Pataki *et al*., 2003).

### *Model parameterization*

The empirical parameters for the photosynthesis and stomatal conductance equations ($m$, $V_m$, and $g_w$) were selected to most accurately simulate carbon and energy fluxes and the foliar $\delta^{13}C$ values measured at the site. Latent heat (*LE*, $W\,m^{-2}$), sensible heat ($H$, $W\,m^{-2}$), net radiation ($R_n$, $W\,m^{-2}$), and *NEE* simulated with different values of $m$, $V_m$, and $g_w$ were compared with the observations using the following two statistics (Collelo *et al*., 1998):

(A) Normalized standard error of the estimate (*NSEE*, dimensionless), which is a dimensionless estimate of relative uncertainty:

$$NSEE = \sqrt{\frac{\sum_{i=1}^{n} (s_i - O_i)^2}{\sum_{i=1}^{n} (O_i)^2}}, \quad (16)$$

where $O_i$ is each half-hourly observation; $s_i$ each half-hourly simulation; and $n$ the number of observations.

(B) *BIAS*: slope of a linear regression line of $(O_i, s_i)$ data pairs.

Ideally, the parameters selected should result in minimum *NSEE* and *BIAS* close to 1 for all the fluxes. Because this study aims to test only vegetation related processes (i.e. photosynthesis and stomatal conductance), we calculated *NSEE* and *BIAS* with daytime values (sunrise to sunset) of selected summer days that had eddy covariance data without gap-filled values, freezing temperatures, and rains (Julian days 200–203, 210–211, and 227–230 of 2000). We selected only summer days because in this period *LE* fluxes would most likely represent tree physiology instead of soil evaporation. The contribution of tree transpiration to total *LE* varies significantly in this site (from 33% to 64% from May to September in 1999–2001), but during the dry late summer, soil evaporation accounted for only 9% of total latent heat flux in a nearby ponderosa pine forest (Irvine *et al*., 2004).

Lack of energy balance closure for the flux data presented a problem for model parameterization, as energy balance closure is enforced in ISOLSM. Eddy flux measurements of *LE*, $H$, and soil heat flux ($G$, $W\,m^{-2}$) for this site in 2000 accounted for about 75–80% of $R_n$. Lack of energy balance closure was also common across 22 flux sites, with mean imbalance of 20% of $R_n$, yet the cause of this imbalance is uncertain (Wilson *et al*., 2002). Overestimation of $R_n$ is not a likely cause of energy closure problems (Anthoni *et al*., 2002) and $G$ is a small component of the energy balance, so we assumed that the imbalance was mainly caused by errors in measurement of *LE* and $H$ fluxes (i.e. because of advection, mesoscale transport, and undetected low frequency contributions to fluxes). Accordingly, each half-hourly measurement of *LE*, $H$, and *NEE* was multiplied by an adjustment factor ($C$, dimensionless), so that $H$ and *LE* summed to the available energy ($R_n - G$) while retaining the observed Bowen ratio ($H/LE$) (Anderson *et al*., 2000):

$$C = \frac{R_n - G}{LE + H}, \quad (17)$$

The *NSEE* and *BIAS* statistics were then calculated for different combinations of parameters using both the unadjusted and adjusted data.

We also calculated the simulated annual integral of photosynthetic discrimination ($\overline{\delta_A}$, ‰), expressed as the flux-weighted annual average $\delta^{13}C$ value of assimilated carbon, for different values of $m$, $V_m$, and $g_w$, and used this value as an additional constraint for parameter estimation.

$$\overline{\delta_A} = \frac{\sum_{i=1}^{n} A_i \delta_{A_i}}{\sum_{i=1}^{n} A_i}, \quad (18)$$

We assumed that $\delta^{13}C$ values of sunlit old leaves collected in Metolius in 2000 and 2001 reflected the long-term photosynthetic discrimination occurring at the site, under a wide range of environmental conditions (i.e. during and outside of the growing season). Therefore, the model parameters selected should result in a simulated $\overline{\delta_A}$ comparable to these foliar $\delta^{13}C$ values.

## Results

### *Parameter estimation*

We used a statistical approach to compare simulations and observations of $R_n$, *LE*, *H*, *NEE*, and $\overline{\delta_A}$ and to select values of parameters $m$ and $V_m$ that produced ISOLSM predictions that best fit measurements from the Metolius site. We conducted multiple test simulations for a selected interval while systematically changing values of $m$ and $V_m$. Statistical metrics (Collelo *et al*., 1998) were calculated that summarized the ability of the simulations to reproduce short-term variation in fluxes (*NSEE*) and to reproduce the magnitude of the fluxes (*BIAS*) when compared with the corresponding observation (Table 3). Ideally, the *NSEE* should be at a minimum and the *BIAS* should approach 1 for all fluxes at the combination of parameter values that give the best fit. As noted by others (Collelo *et al*., 1998), it was not possible to find a unique combination of these parameters that gave minimum errors in fits to *LE*, *H*, and *NEE* alone (i.e. in the absence of using the isotope measurements). Rather the two parameters, $m$ and $V_m$, tended to trade off. For example, similar fits to unadjusted *LE* could be obtained with $m = 12$, $V_m = 25$; $m = 10$, $V_m = 40$; and $m = 8$, $V_m = 55$, and to adjusted *NEE* with $m = 12$, $V_m = 55$; and $m = 10$, $V_m = 70$ (Table 3). Fits using the unadjusted fluxes gave larger errors and somewhat lower parameter values.

As an additional constraint on the selection of parameters we calculated the flux-weighted average carbon isotope ratio, $\overline{\delta_A}$, for gross photosynthetic $CO_2$ uptake over a full year for comparison with the measured foliar $\delta^{13}C$ values observed at the site (shown as the dashed line, Fig. 1). Interestingly, the simulations show that the value of $\overline{\delta_A}$ was relatively independent of the $V_m$ and strongly dependent on the value of $m$ used in the

**Table 3** *NSEE* and *BIAS* statistics of observed vs. simulated carbon and energy fluxes (*H*, *LE*, and *NEE*)

| | $V_m$ | 25 | 40 | 55 | 70 | 90 |
|---|---|---|---|---|---|---|
| | ***m*** | | | | | |
| *(a) Unadjusted data* | | | | | | |
| ***H*** | | | | | | |
| *NSEE* | **8** | | 0.56 | 0.52 | 0.48 | 0.43 |
| | **10** | 0.56 | 0.49 | 0.42 | 0.37 | 0.35 |
| | **12** | 0.51 | 0.42 | 0.37 | 0.40 | |
| *BIAS* | **8** | | 1.16 | 1.14 | 1.11 | 1.07 |
| | **10** | 1.15 | 1.11 | 1.02 | 0.95 | 0.85 |
| | **12** | 1.12 | 1.02 | 0.88 | 0.74 | |
| ***LE*** | | | | | | |
| *NSEE* | **8** | | 0.44 | 0.40 | 0.37 | 0.40 |
| | **10** | 0.43 | 0.37 | 0.47 | 0.65 | 0.90 |
| | **12** | 0.40 | 0.50 | 0.82 | 1.15 | |
| *BIAS* | **8** | | 0.71 | 0.60 | 0.56 | 0.64 |
| | **10** | 0.70 | 0.56 | 0.69 | 0.88 | 1.09 |
| | **12** | 0.63 | 0.69 | 0.99 | 1.25 | |
| ***NEE*** | | | | | | |
| *NSEE* | **8** | | 0.64 | 0.51 | 0.51 | 0.61 |
| | **10** | 0.74 | 0.54 | 0.38 | 0.55 | 0.95 |
| | **12** | 0.76 | 0.42 | 0.41 | 0.85 | |
| *BIAS* | **8** | | 0.31 | 0.62 | 0.91 | 1.17 |
| | **10** | 0.17 | 0.46 | 0.83 | 1.17 | 1.49 |
| | **12** | 0.14 | 0.54 | 1.00 | 1.32 | |
| *(b) Adjusted data* | | | | | | |
| ***H*** | | | | | | |
| *NSEE* | **8** | | 0.17 | 0.16 | 0.16 | 0.18 |
| | **10** | 0.17 | 0.16 | 0.21 | **0.26** | 0.35 |
| | **12** | 0.16 | 0.22 | 0.32 | 0.44 | |
| *BIAS* | **8** | | 1.06 | 1.03 | 1.00 | 0.96 |
| | **10** | 1.06 | 1.01 | 0.94 | 0.87 | 0.79 |
| | **12** | 1.03 | 0.94 | 0.83 | 0.70 | |
| ***LE*** | | | | | | |
| *NSEE* | **8** | | 0.48 | 0.40 | 0.35 | 0.30 |
| | **10** | 0.48 | 0.37 | 0.30 | **0.31** | 0.43 |
| | **12** | 0.40 | 0.33 | 0.41 | 0.60 | |
| *BIAS* | **8** | | 0.53 | 0.52 | 0.48 | 0.54 |
| | **10** | 0.51 | 0.45 | 0.54 | 0.71 | 0.88 |
| | **12** | 0.49 | 0.52 | 0.77 | 1.00 | |
| ***NEE*** | | | | | | |
| *NSEE* | **8** | | 0.74 | 0.60 | 0.48 | 0.38 |
| | **10** | 0.84 | 0.66 | 0.42 | **0.27** | 0.40 |
| | **12** | 0.84 | 0.56 | 0.27 | 0.35 | |
| *BIAS* | **8** | | 0.22 | 0.45 | 0.67 | 0.85 |
| | **10** | 0.09 | 0.33 | 0.57 | 0.79 | 0.96 |
| | **12** | 0.10 | 0.37 | 0.63 | 0.81 | |

The simulated values were obtained with different values of the parameters $m$ and $V_m$, and then compared with the unadjusted and adjusted (for energy balance closure) eddy flux data. For each combination of parameters ($m$ and $V_m$), the statistics calculated with the unadjusted data are given in Table 3a, and those calculated with adjusted data are given in Table 3b.

simulations (Fig. 1). This parameter is the slope of the relationship between stomatal conductance and the rate of $CO_2$ assimilation (scaled by humidity and $CO_2$ concentration, Eqn (6)). All else remaining equal, changing this parameter should change the ratio of chloroplast to ambient $CO_2$ concentration, and this, in turn, determines the carbon isotope discrimination. Nevertheless, it is surprising that this holds when integrated over a full year. The simulated variables were also sensitive to mesophyll wall conductance, especially at low values of $g_w$ ($g_w < 3000V_m$) (Fig. 2). We have no direct measurements of this parameter for *P. ponderosa*. The sensitivity analyses mentioned above and the remainder of the simulations were performed with $g_w = 4800V_m$, which is comparable to values reported by Evans and Loreto (2000) for other species.

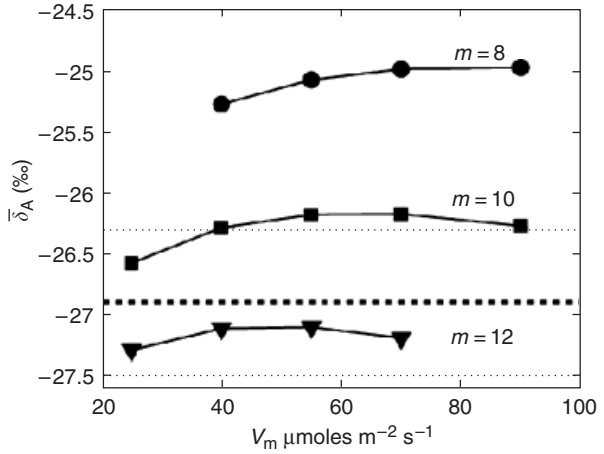


**Fig. 1** Sensitivity of the annual flux-weighted average of simulated photosynthetic carbon isotope discrimination, $\overline{\delta_A}$, to $V_m$ (*x*-axis) and *m*. Circles: $m = 8$; squares: $m = 10$; triangles: $m = 12$. Mean $\delta^{13}C$ value of old leaves collected in 2000 and 2001 is indicated by the dashed line (−26.9‰), and its standard deviation by the dotted line (0.6‰).

The $\delta^{13}C$ values of sunlit old leaves collected in Metolius during 2000 and 2001 gave a mean value of −26.9‰ (standard deviation = 0.6‰, $n = 15$), while young sunlit leaves and old shaded leaves had somewhat lower $\delta^{13}C$ values (−28.5‰ ± 1.1, $n = 4$; and −27.7‰ ± 0.9, $n = 5$, for young sunlit and old shaded leaves, respectively) (data available in BASIN: http://basinisotopes.org). If we assume that most of the photosynthesis is made by sunlit leaves, and that fixed carbon was used without further fractionation as the substrate for respiration and growth of new plant tissues, then we

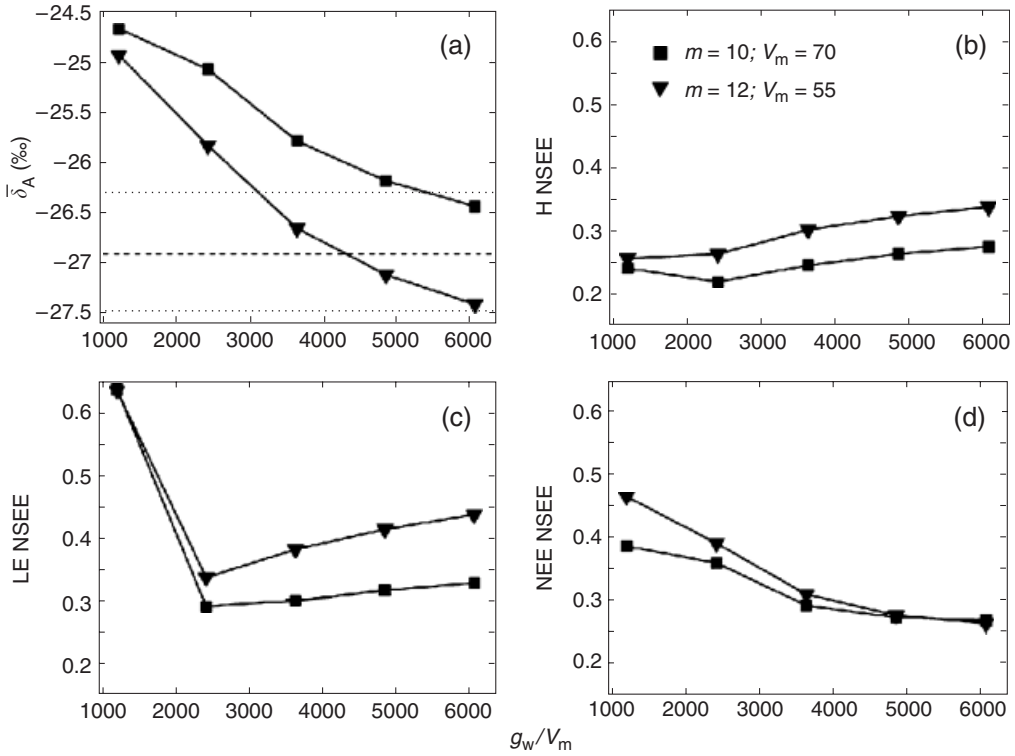


**Fig. 2** Sensitivity of simulated $\overline{\delta_A}$, carbon, and energy fluxes to mesophyll wall conductance ($g_w$). The *x*-axis represents different values of the proportionality constant of the mesophyll wall conductance equation (Eqn (5)): $g_w/V_m$. The different symbols indicate simulations with different combinations of parameters: squares: $m = 10$ and $V_m = 70\,\mu mol\,m^{-2}\,s^{-1}$; triangles: $m = 12$ and $V_m = 55\,\mu mol\,m^{-2}\,s^{-1}$. a) simulated $\overline{\delta_A}$. The dashed line represents the mean $\delta^{13}C$ of old leaves collected at the site, and the dotted line is the standard deviation. b, c, and d) *NSEE* of *H*, *LE* and *NEE* respectively, calculated with adjusted eddy flux data.

may estimate that the value of $m$ is between 10 and 12 (Fig. 1). We considered this constraint together with the constraints imposed by the flux observations and chose $m = 10$, $V_m = 70$ for the adjusted fluxes and $m = 10$, $V_m = 55$ for the unadjusted data set. An $m$ value of 12 provides a better fit to the foliar $\delta^{13}C$ data, but the $V_m$ value that minimizes *NSEE* of the adjusted fluxes for that $m$ is 55, much lower than values obtained at the site with $A/c_i$ curves ($V_m = 73$) (Law *et al.*, 2000), and the *NSEE* for both *LE* and *H* were higher than for $m = 10$ and $V_m = 70$. Therefore, we selected $m = 10$, and the $V_m$ value that best fitted the adjusted *H*, *LE*, and *NEE* data for that $m$ was $V_m = 70$ (Table 3). We acknowledge that it would be possible to use a more sophisticated approach to arrive at an optimal fit. However, it seems unlikely that the quality of the fit could be greatly improved, given the large scatter and incomplete energy balance closure of the eddy covariance data.

### *Comparison of simulated fluxes and discrimination to observations*

Time series plots of fluxes of *LE* and *NEE* for several selected days using the selected parameters are shown in Figs. 3 and 4. Corresponding 1 : 1 plots of simulated values vs. observations are shown in Fig. 5. Plots of simulated values and observations of net radiation are not shown. As measurements of $R_n$ were used to derive the radiation fluxes used to force the model, the nearly perfect agreement between observations and simulations

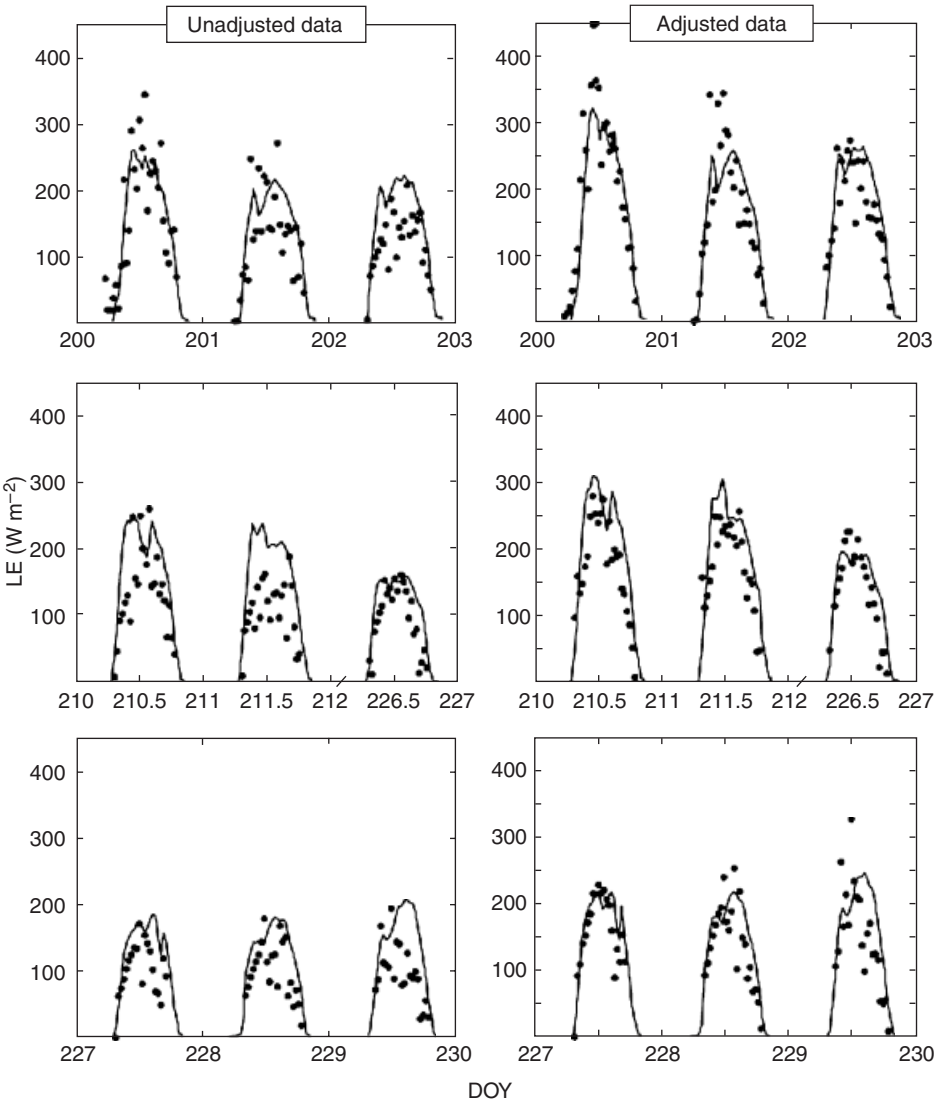


**Fig. 3** Time series of observed and simulated *LE*. The left-hand side panels represent unadjusted observations (dots) and simulated values (solid lines) obtained with $m = 10$ and $V_m = 55\,\mu mol\,m^{-2}\,s^{-1}$. The right-hand side panels represent adjusted observations for energy balance closure (dots) and simulated values (solid lines) obtained with $m = 10$ and $V_m = 70\,\mu mol\,m^{-2}\,s^{-1}$. Doy indicates the day of the year.

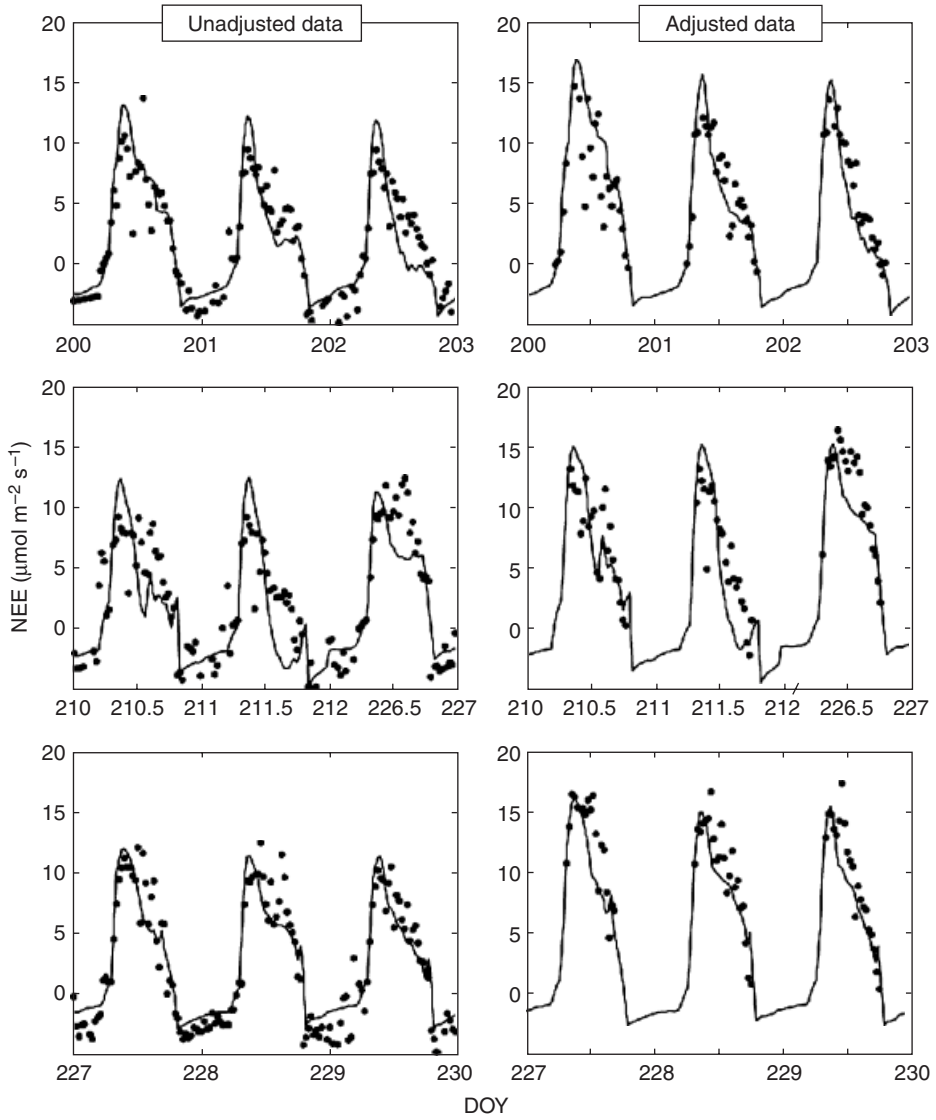


**Fig. 4** Time series of observed and simulated *NEE*. The left-hand side panels represent unadjusted observations (dots) and simulated values (solid lines) obtained with $m = 10$ and $V_m = 55\,\mu mol\,m^{-2}\,s^{-1}$. The right-hand side panels represent adjusted observations for energy balance closure (dots) and simulated values (solid lines) obtained with $m = 10$ and $V_m = 70\,\mu mol\,m^{-2}\,s^{-1}$. Doy indicates the day of the year.

is trivial. The adjusted fluxes of *H*, *LE*, and *NEE* clearly increased relative to the unadjusted fluxes (Figs. 3 and 4), and, more significantly, the model was able to simulate the adjusted fluxes with less scatter than the unadjusted fluxes (Fig. 5), yielding more accurate parameter estimation. Using a different set of parameters for the unadjusted data did not improve the fits, as shown by the generally larger *NSEE* in Table 3.

The time course of the simulated $\delta^{13}C$ of the daily integral of carbon uptake and carbon respired through the 2001 growing season is shown in Fig. 6. These time courses are remarkable for the large coherent variation in isotope ratio that is presumably related to the weather patterns of that year. During mid-season (days 184–191), $CO_2$ respired by leaves was collected (McDowell *et al.*, 2004a), which we assume was drawn from recent assimilates. The $\delta^{13}C$ of this $CO_2$ varied substantially over the sampling interval and this variation was similar to the simulated changes in carbon uptake over that time ($\delta_A$) (Fig. 6a). We assumed that ecosystem respiration (Fig. 6b) was a mixture of recent assimilates (with a lag of 1 day for carbon to be transported to the roots), and decomposition of soil organic matter. The latter is assumed to have a constant $\delta^{13}C$ value (−26.2‰), consequently, the variation in $\delta_R$ is attenuated relative to that of $\delta_A$ (Fig. 6).

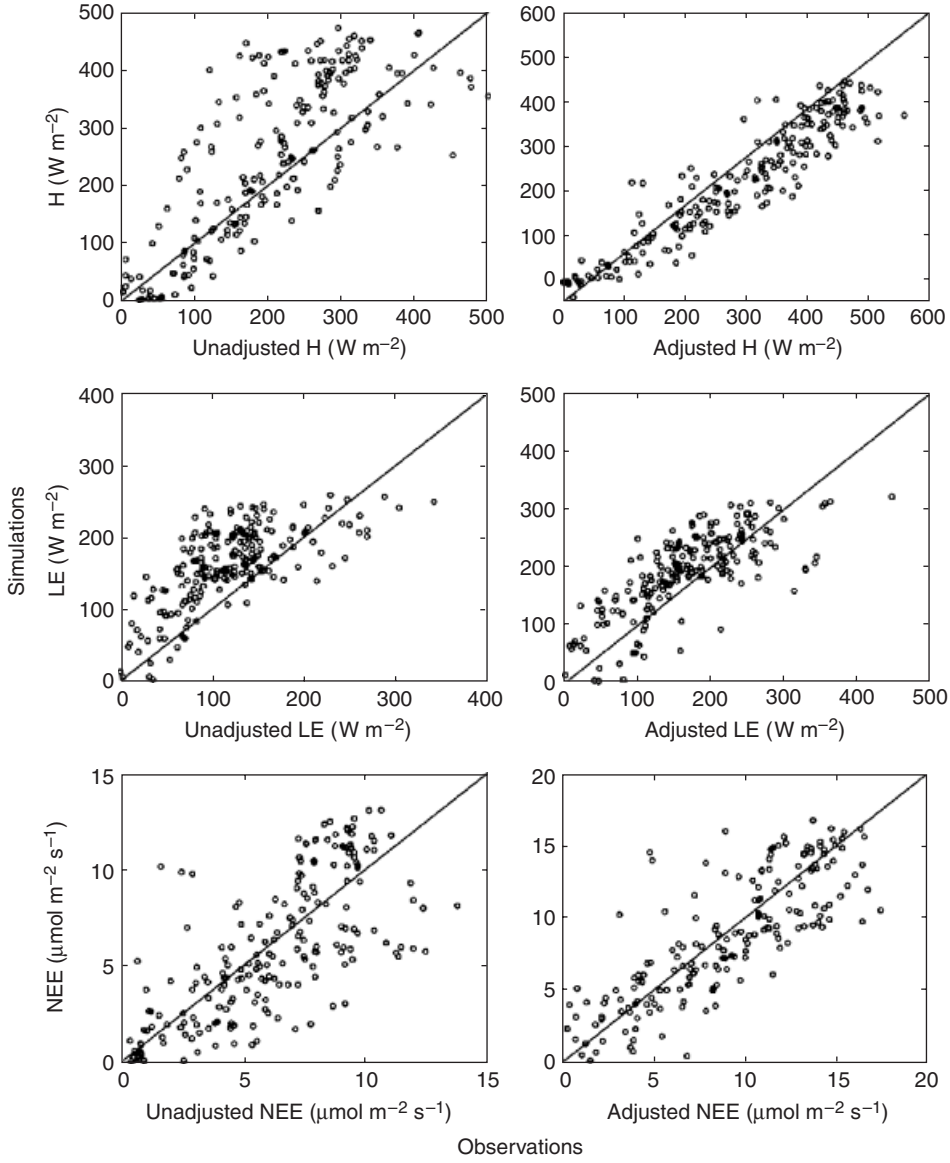


**Fig. 5** One-to-One plots of half-hourly observations (*x*-axis) vs. simulations (*y*-axis) for *H*, *LE*, and *NEE*. Left-hand side panels: unadjusted observations vs. simulated values obtained with $m = 10$ and $V_m = 55\,\mu mol\,m^{-2}\,s^{-1}$. Right-hand side panels: adjusted observations (for energy balance closure) vs. simulated values obtained with $m = 10$ and $V_m = 70\,\mu mol\,m^{-2}\,s^{-1}$.

Samples of air from the canopy air space were collected at night over the same interval and analyzed by Keeling plots to estimate the isotopic composition of ecosystem respiration, (diamonds, Fig. 6, data from McDowell *et al*., 2004a). These values also matched the simulated values reasonably well, although the variation in these data points is smaller than the simulated variation. Bowling *et al*. (2002) proposed that the variation in $\delta_R$ in this and other forests in Oregon was correlated to variation in the *VPD* several days before the measurement time. The daily integral of $\delta_A$ and night-time $\delta_R$ are plotted vs. the *VPD* of the corresponding days in Figs. 7 and 8 respectively, showing that a large variation in $\delta_A$ and $\delta_R$ in the simulations is associated with variation in *VPD*. This correlation is most likely associated with rainfall events and movement of high and low pressure systems over the site. Most of the measurements of leaf respiration (squares, Fig. 7) plotted at the mean *VPD* of the corresponding day fall within the range of simulated values. The lowest $\delta_f$ value, located much below the range of simulations (day 184 in Fig. 6) seems to track the low isotopic signature of photosynthesis a few days before. The dashed line in Figs. 7 and 8 is the empirical

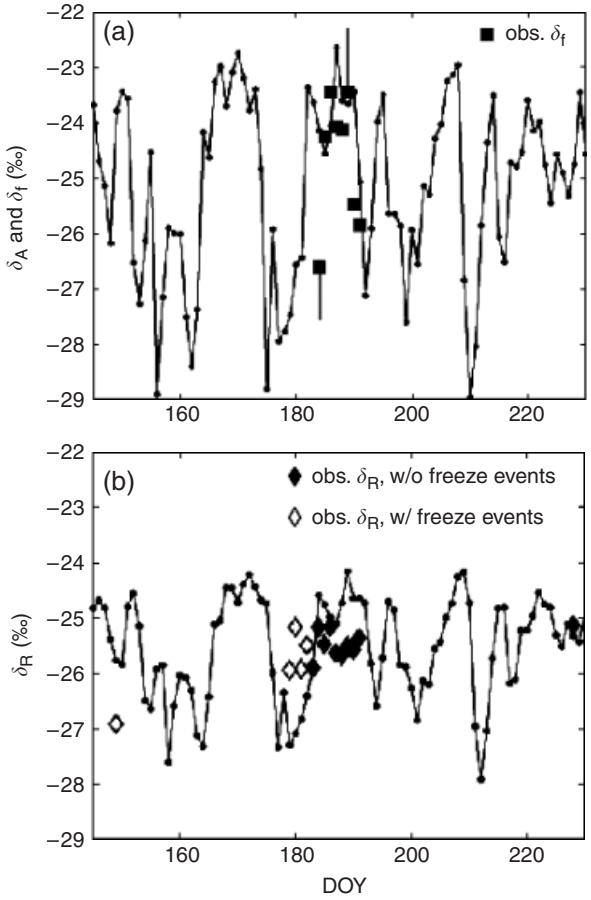


**Fig. 6** Time series of simulated and observed $\delta^{13}C$ values for 2001. Each symbol represents a flux-weighted daily-averaged value. (a) Simulated $\delta_A$ (dots) and observed $\delta_f$ (squares). Bars indicate standard errors of the estimate. (b) Simulated $\delta_R$ (dots), $\delta_R$ measured during freeze events (minimum air temperature $<0.2\,^{\circ}C$ in the last 7 days) (open diamonds), and $\delta_R$ measured during periods without freeze events (filled diamonds). Standard errors for observed $\delta_R$ varied from 0.1‰ to 0.4‰. Respiration data are from McDowell *et al*. (2004a).

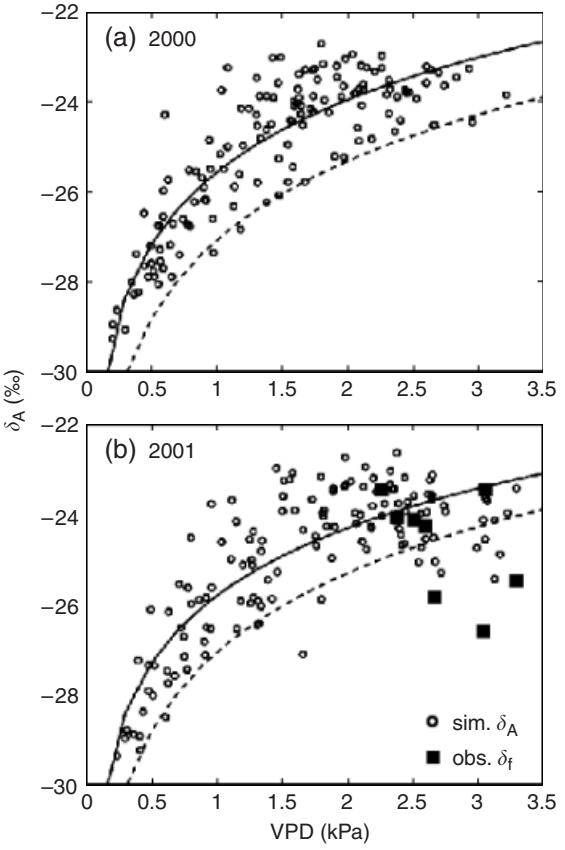


**Fig. 7** Relationship between *VPD* and simulated flux-weighted daily-averaged $\delta_A$ ($\delta_A$, circles) over the growing season (days 130–270). The dashed lines represent the relationship between *VPD* and $\delta_R$ reported in Bowling *et al*. (2002): $y = 2.54\ln(x) - 27.08$; $r^2 = 0.79$; $n = 22$. The solid lines are logarithmic fits to *VPD* vs. simulated $\delta_A$. (a) Year 2000. $y = 2.325\ln(x) - 25.57$; $r^2 = 0.76$. (b) Year 2001. $y = 2.17\ln(x) - 25.82$; $r^2 = 0.71$. the squares represent $\delta_f$ measured by McDowell *et al*. (2004a) in 2001.

relationship between $\delta_R$ and *VPD* found by Bowling *et al*. (2002). The diamonds in Fig. 8a are $\delta_R$ values obtained in year 2000 plotted using the *VPD* 5 days previous to the measurement. Fig. 8b shows a similar plot with $\delta_R$ values collected in 2001 in the same site (McDowell *et al*. 2004a) against *VPD* of the previous day. While they did not observe a strong correlation with *VPD* in their 2001 data, it is evident that their points fall within the range of the corresponding simulations.

McDowell *et al*. (2004a,b) emphasized the possible role of other environmental and physiological factors in affecting foliar and ecosystem respiration. We used linear regression analysis to examine possible correlations between simulated $\delta_A$ and $\delta_R$ and several forcing and meteorological variables described by McDowell *et al*. (2004a,b). Table 4 shows that there are many strong correlations with soil and air temperature, soil moisture, radiation, photosynthetic uptake, and stomatal conductance. Radiation and air temperature are driving factors of the photosynthesis and stomatal conductance model, so their correlation with discrimination reflects these physiological interactions. Soil moisture and temperature, however, were decoupled from the physiological component of the model (photosynthesis, stomatal conductance, and discrimination), because we assumed that trees had permanent access to deep groundwater. The correlation between soil variables and simulated $\delta_A$ and $\delta_R$ may only result from the covariation among soil and atmospheric variables, the latter determining discrimination. For example, radiation, air temperature and humidity (which determine discrimination), soil temperature, and soil moisture tend to be associated in this site, which mostly lacks summer precipitation.

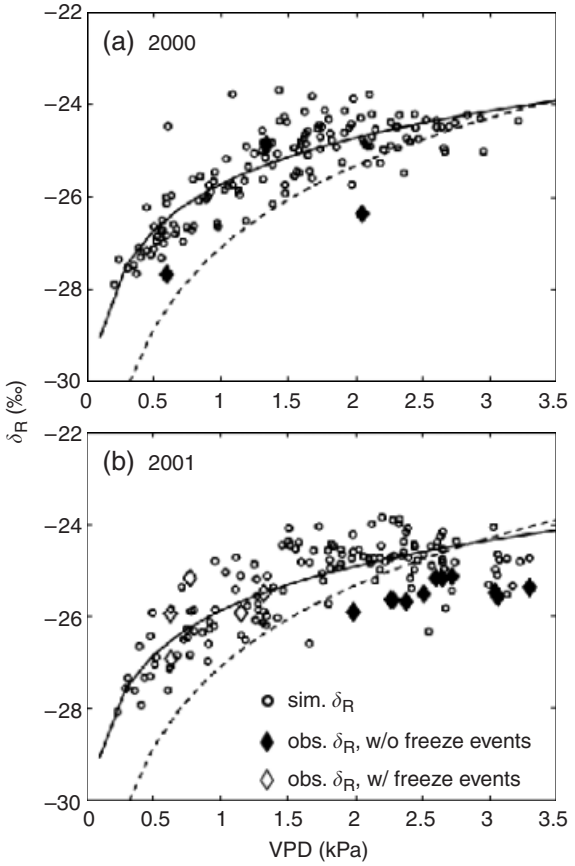


**Fig. 8** Relationship between *VPD* and flux-weighted daily-averaged simulated (circles) and observed (diamonds) $\delta_R$, over the growing season (days 130–270). The dashed lines represent the relationship between *VPD* and $\delta_R$ reported in Bowling *et al.* (2002): $y = 2.54\ln(x) - 27.08$; $r^2 = 0.79$; $n = 22$. The solid lines are logarithmic fits to *VPD* vs. simulated $\delta_R$. (a) Year 2000. $y = 1.44\ln(x) - 25.72$; $r^2 = 0.74$. Diamonds represent $\delta_R$ measured in 2000 and plotted against *VPD* lagged 5 days (as reported in Bowling *et al.*, 2002). (b) Year 2001. $y = 1.33\ln(x) - 25.87$; $r^2 = 0.65$. Open diamonds indicate $\delta_R$ measurements obtained during freeze events (minimum air temperature $< 0.2\,^{\circ}C$ in the last 7 days). Filled diamonds indicate measurements obtained outside freeze events. The 2001 $\delta_R$ data are plotted against *VPD* of the previous day.

**Table 4** Relationships between different environmental factors and simulated $\delta^{13}C$ during different sampling periods

| X | Y | Sampling time, days of the year | $r^2$ | $P$ | Sign of relationship |
|---|---|---|---|---|---|
| Radiation | $\delta_A$ | 130–270 | 0.71 | <0.0001 | + |
| Radiation | $\delta_R$ | 130–270 | 0.34 | <0.0001 | + |
| Radiation | $\delta_A$ | 10–365 | 0.90 | <0.0001 | + |
| Radiation | $\delta_R$ | 10–365 | 0.69 | <0.0001 | + |
| $A$ | $\delta_A$ | 130–270 | 0.00 | 0.5064 | |
| $A$ | $\delta_A$ | 10–365 | 0.68 | <0.0001 | + |
| $G_c$ | $\delta_A$ | 130–270 | 0.72 | <0.0001 | − |
| $G_c$ | $\delta_R$ | 130–270 | 0.44 | <0.0001 | − |
| $G_c$ | $\delta_A$ | 10–365 | 0.03 | 0.0017 | + |
| $G_c$ | $\delta_R$ | 10–365 | 0.02 | 0.0027 | + |
| Air temperature | $\delta_A$ | 130–270 | 0.50 | <0.0001 | + |
| Air temperature | $\delta_R$ | 130–270 | 0.48 | <0.0001 | + |
| Air temperature | $\delta_A$ | 10–365 | 0.76 | <0.0001 | + |
| Air temperature | $\delta_R$ | 10–365 | 0.71 | <0.0001 | + |
| Soil moisture | $\delta_A$ | 130–270 | 0.18 | <0.0001 | − |
| Soil moisture | $\delta_R$ | 130–270 | 0.27 | <0.0001 | − |
| Soil moisture | $\delta_A$ | 10–365 | 0.36 | <0.0001 | − |
| Soil moisture | $\delta_R$ | 10–365 | 0.37 | <0.0001 | − |
| Soil temperature | $\delta_A$ | 130–270 | 0.35 | <0.0001 | + |
| Soil temperature | $\delta_R$ | 130–270 | 0.47 | <0.0001 | + |
| Soil temperature | $\delta_A$ | 10–365 | 0.66 | <0.0001 | + |
| Soil temperature | $\delta_R$ | 10–365 | 0.72 | <0.0001 | + |

X and Y indicate the two variables correlated, sampling time indicates the time period included in the correlations, $r^2$ is the coefficient of determination of a linear regression analysis, $P$ indicates significance, and the sign of the relationship indicates whether it is positive or negative. Soil moisture and soil temperature did not have any control on simulated discrimination, whereas the other factors directly or indirectly controlled simulated discrimination, and indeed $\delta_A$ and $\delta_R$.

## Discussion

### *Parameter estimation using eddy fluxes and isotopic measurements*

Combining eddy fluxes with isotope measurements to constrain the estimation of the parameters $m$ and $V_m$ resulted in a smaller parameter space than using the eddy fluxes alone. Several problems emerged from both data sets (eddy fluxes and isotopes), but we contend that these can be resolved with future measurements, making isotope measurements useful to constrain land surface models.

Eddy flux measurements commonly lack energy balance closure (Wilson *et al.*, 2002), while the model enforces it in the simulated fluxes. This makes comparisons between model and data difficult, because the causes of the lack of energy balance closure are not well understood and cannot be included in the model. As an alternative approach, we applied an adjustment factor to the eddy flux data, assuming that the imbalance is mainly caused by errors in the measurements of *LE* and *H* ($LE + H = R_n - G$). We acknowledge that this adjustment may bias the fluxes, but we preferred to use the adjusted data in this case because using unadjusted eddy flux measurements to search for an optimum fit of simulated *LE*, *H*, and *NEE* fluxes did not provide a

consistent set of parameters ($m$ and $V_m$) that simultaneously optimized all the fluxes (i.e. $m = 10$, $V_m = 55$ fit *NEE* but not *LE* and *H*) (Table 3). Using the adjusted data provided a more consistent fit of all the fluxes and reduced the dispersion of observed vs. simulated values (Fig. 5), resulting in generally lower *NSEE* (Table 3).

However, the optimization using the adjusted eddy fluxes yielded a range of values for $m$ and $V_m$ that resulted in similar fits. Increasing the value of $V_m$ while decreasing the value of $m$ could provide similarly low *NSEE* (i.e. both $m = 12$, $V_m = 55$; and $m = 10$, $V_m = 70$ minimized *NSEE* of *NEE* calculated with the adjusted fluxes). We found that carbon isotope discrimination could further constrain the model parameterization, because it is more strongly sensitive to the stomatal conductance parameter, $m$, than to $V_m$ (Fig. 1). The annual integral of carbon isotope ratios of assimilates, $\overline{\delta_A}$, was sensitive to different values of $m$ but it was relatively independent from $V_m$. In this context, carbon isotope measurements should impose a constraint on the model, if we could measure the integrated canopy discrimination at similar spatial and temporal scales as the simulated discrimination. Several measurements reflect photosynthetic carbon isotope discrimination: $\delta^{13}C$ of plant carbon, leaf and phloem sugars, foliar and ecosystem respiration (Keitel *et al*., 2003; Pataki *et al*., 2003; Barbour *et al*., 2005; Mortazavi *et al*., 2005). However, these measurements may be affected by isotope fractionation during other processes (i.e. respiration), and it is difficult to determine the time period at which the carbon present in the sample was fixed. In the Metolius site, only $\delta^{13}C$ values of leaves, ecosystem, and foliar respiration were available. We selected foliar $\delta^{13}C$ data to optimize the model parameters and reserved the $\delta^{13}C$ values of respiration to test the model. Foliar $\delta^{13}C$ integrates all the processes affecting carbon discrimination during the leaf lifetime, which in this site is 2–3 years. Leaf growth occurs between May to August, and 50–70% of carbon fixation occurs outside of the growing season (Law *et al*., 2000). Respiratory fractionation is unlikely to significantly contribute to the carbon isotope composition of plant biomass (Ghashghaie *et al*., 2003). Therefore, we assumed that foliar $\delta^{13}C$ represents the long-term (annual) isotope discrimination of the site.

There can be significant variations of photosynthetic activity between leaves of different age or located at different positions in the canopy. We tried to reduce these errors by using data from sunlit old leaves, because most of the photosynthesis at this site is conducted by sun leaves in the upper canopy, and old leaves should represent a wider range of environmental conditions than young leaves. For comparison, the model calculated an integrated annual value of $\delta_A$ ($\overline{\delta_A}$) for the whole canopy, which should approximate the foliar $\delta^{13}C$ values selected. This agreement occurred with $m$ values between 10 and 12 (Fig. 1), which are higher than values previously used for conifers at this and other sites ($m = 6$, Bonan, 1996; $m = 7.4$, Kurpius *et al*., 2003; $m = 8$, Law *et al*., 2000; Law *et al*., 2001a). Using the isotope data to constrain the parameter $m$ reduced the range of parameters obtained with the eddy fluxes by eliminating low values of $m$. Although $m = 12$ would provide the best fit to the isotope data (Fig. 1), the $V_m$ values that reduced the flux errors for that $m$ ($V_m = 55$ or lower, Table 3) are much lower than those estimated at the site with $A/c_i$ curves ($V_m = 73$) (Law *et al*., 2000) and result in higher *NSEE* for the energy fluxes. Therefore, we selected $m = 10$, and the $V_m$ value that best fitted the adjusted *H*, *LE*, and *NEE* data for that $m$ was $V_m = 70$ (Table 3). We acknowledge that the metrics we selected to quantify ecosystem isotope balance are still open to discussion, but these issues can be resolved with better measurements of photosynthetic discrimination that are comparable in time and space to model estimates. For example, $\delta^{13}C$ values of young leaves of known age or leaf sugars, or direct measurements of isotope discrimination could be compared with simulated $\delta_A$ obtained with the meteorology of a corresponding time period, to better constrain the parameter estimation.

Time series of simulated *LE* and *NEE* with the selected parameters ($m = 10$ and $V_m = 70$) reasonably matched the adjusted data (Figs. 3 and 4). *LE* fluxes presented similar midday depressions as those observed and simulated at the leaf level, which result from interactions among leaf boundary layer conductance, air humidity and temperatures, stomatal conductance, and photosynthetic rates (Collatz *et al*., 1991; Anthoni *et al*., 1999). This shows that including the capacity to simulate isotope discrimination together with a few simple isotopic measurements can lead to improvements in the ability of the model to simulate other processes involved in the carbon and energy balance of the ecosystem.

### *Model testing*

Isotope discrimination is apparently helpful in fitting the model predictions to the measured fluxes, but we caution that it could be possible to accurately simulate the yearly integral of leaf $\delta^{13}C$ without accurately simulating the responses of discrimination to environmental variation. To check the performance of the model in this time domain, we used measurements of the isotopic composition of respired $CO_2$ obtained during a different year from the eddy flux measurements used to calibrate the model. We assumed that leaf respiration tracks assimilation, and that ecosystem respiration is a composite of autotrophic respiration

from leaves, roots, and stems drawn from recent photosynthesis (with a 1 day lag for root and stem respiration), and heterotrophic respiration from bulk soil organic matter with a constant $\delta^{13}C$. We ignored the effects of respiration on the isotope ratio of the respired C, because the net effect of fractionation during different respiratory processes in uncontrolled conditions at the ecosystem level is poorly understood. For example, consumption of sucrose results in $CO_2$ that is enriched in $^{13}C$ by 2–6‰, while photorespiration may produce $CO_2$ depleted in $^{13}C$ by 8–11‰, and both processes vary in strength with species and environmental conditions (Ghashghaie *et al*., 2003; Klumpp *et al*., 2005). It is not clear either how fractionation during microbial respiration of soil organic matter would affect the soil $CO_2$ efflux, or which organic matter pools are respired.

The simulated $\delta_R$ varied by about 3‰ and $\delta_A$ by about 5‰ over the same period of $\delta_R$ and $\delta_f$ observations. The $\delta_R$ and $\delta_f$ measurements were close to the corresponding simulated values and in some cases the variations in the measurements tracked the variation in the simulations (Fig. 6). The $\delta_f$ measurement taken on day 184 does not fit the corresponding simulated value for the same day, but has a high standard error and seems to reflect the low discrimination values of a few days before (Fig. 6a). Most of the observed $\delta_f$ values plotted against *VPD* (Fig. 7b) fall within the simulated $\delta_A$ values using the actual meteorology (except for the lowest $\delta_f$ value on day 184, Fig. 6a). The similarity of the daily variability of simulated $\delta_A$ and observed $\delta_f$ was remarkable (Fig. 6a), suggesting that measurements of $\delta_f$ track the short-term variations of photosynthetic discrimination. This agrees with $\delta_f$ measurements obtained by Mortazavi *et al*. (2005) in pine and hardwood forests, which also tracked the variability of expected $\delta_A$ better than other respiratory components.

It is also significant that the pattern of the simulated response of $\delta_R$ to *VPD* was very similar to an empirical relationship found for observed $\delta_R$ (Bowling *et al*., 2002; dashed lines of Fig. 8). This analysis demonstrates the plausibility of a hypothesis first proposed by Bowling *et al*. (2002), that links synoptic cycles of the weather to variations in ecosystem respiration observed at the site. However, the simulated daily variability of $\delta_R$ was higher than that of observed $\delta_R$ (Fig. 6). Our model is incomplete in that we do not explicitly simulate respiration and the dynamics of carbon flow through the ecosystem, therefore, discrepancies between simulated and measured $\delta_R$ values were expected. We assumed a constant lag of 1 day between assimilation and root respiration of assimilates, but recent studies have shown that the degree of coupling between photosynthesis and respiration (with lag times between less than 1 and 5 days) may vary with environmental conditions and for different ecosystems (Scartazza *et al*., 2004; Barbour *et al*., 2005; Knohl *et al*., 2005). Different isotopic signatures of soil organic carbon pools respired by microorganisms, the effect of canopy processes on root respiration, fractionation during microbial respiration, and the effect of freezing temperatures on the proportional contribution of soil organic matter to ecosystem respiration were not included in the model, because the understanding of these processes at the ecosystem scale is rudimentary (Bowling *et al*., 2002; Lai *et al*., 2004; Irvine *et al*., 2005; Tu & Dawson, 2005). The simulations of $\delta_A$ provided by ISOLSM, together with continuous ecosystem measurements of respiration can be useful to study these and other carbon cycle processes occurring in ecosystems.

Although our study focused on the canopy scale of a semi-arid pine forest, the equations used for photosynthesis and stomatal conductance in ISOLSM are also used in multilayer canopy models (CANISOTOPE, Baldocchi & Bowling, 2003; ACASA, Pyles *et al*., 2000) and in larger scale simulations (i.e. LSM, Bonan, 1996; MM5/ISOLSM, Cooley *et al*., 2005; Riley *et al*., 2005; SiB2, Sellers *et al*., 1996). In addition, ISOLSM is used to simulate global patterns of $^{18}O$ in $CO_2$ (Noone *et al*., 2002). Global simulations of the temporal variability of terrestrial ecosystem discrimination are needed to estimate the magnitude of the terrestrial carbon sink, because interannual changes of discrimination, i.e. related to increased drought stress during ENSO events, significantly affect these estimates (Ropelewski & Halpert, 1996; Randerson *et al*., 2002; Scholze *et al*., 2003; Randerson, 2005). Previous regional to global scale simulations incorporating $C_3$ isotope discrimination have been driven by long-term average meteorology, meteorology from reanalysis products, global circulation models, and remote sensing data (Fung *et al*., 1997; Buchmann & Kaplan, 2001; Kaplan *et al*., 2002; Scholze *et al*., 2003; Still *et al*., 2003; Suits *et al*., 2005). These studies provided useful insights about regional and temporal patterns of isotope discrimination. However, the temporal and spatial scales that the available isotopic measurements and the simulations represented were not well suited to test the capacity of these models to simulate the response of terrestrial isotope discrimination to short-term environmental fluctuations. The availability of meteorological, eddy flux, and isotope data in the Metolius site allowed us to calibrate and test ISOLSM with multiple constraints, and validate the treatment of $C_3$ photosynthetic discrimination in response to short-term environmental conditions. Therefore, we show that ecosystem isotope measurements (some available through the BASIN network: http://basinisotopes.org) can be very valuable to test land surface and carbon balance models and to estimate the variability of terrestrial ecosystem discrimination.

*Relationships between environmental and physiological variables and discrimination*

Several studies relate the variability of $\delta^{13}C$ of different ecosystem components to environmental conditions (McDowell *et al*., 2004a, b; Scartazza *et al*., 2004; Knohl *et al*., 2005; Mortazavi *et al*., 2005). It is often difficult to interpret the underlying mechanisms of the observed variations, and even to determine the sampling frequency required to capture the main controls on ecosystem $\delta^{13}C$, because numerous processes act on $^{13}C$ discrimination at different spatial and temporal scales (e.g. short-term changes of photosynthetic discrimination, transport and allocation of carbohydrates, respiration of C pools of different ages). Modeling allows us to analyze these issues because we can determine the processes simulated and the temporal scales analyzed, and then compare simulated and observed patterns of discrimination. Here, we describe similar relationships between environmental conditions and simulated $\delta_A$ and $\delta_R$ as those observed by McDowell *et al*. (2004a,b) for $\delta_f$ and $\delta_R$ in the same region. It is not surprising that several atmospheric and physiological variables that were correlated to the observations (McDowell *et al*., 2004a,b) were also correlated in our simulations, as ISOLSM reflects the nonlinear controls of atmospheric conditions (i.e. wind speed, radiation, relative humidity, and air temperature) on stomatal conductance and photosynthesis (Eqns (1)–(3) and (6)). Table 4 shows that we could find many correlations between discrimination and environmental and physiological variables (i.e. radiation, photosynthesis, air temperature, canopy conductance, soil temperature, and soil moisture). Although we do not know the mechanistic relationships that may underlie such correlations in nature, the model defines these relationships in the simulations. We know that some variables such as soil moisture and soil temperature should not affect $\delta_A$ in these simulations – as ISOLSM was constrained to ignore soil moisture information. Nevertheless, soil moisture and temperature showed a significant correlation with $\delta_A$, which must be the result of a secondary correlation in the environmental data. This result argues for the possibility that similar indirect correlations might appear in nature.

Similarly, the analysis showed that clear causal relationships coded in the model may not show up in correlation analysis during particular sampling periods. For example, photosynthesis was not correlated to $\delta_A$ during the growing season, when significant variations of stomatal conductance controlled discrimination. Canopy conductance was not correlated to $\delta_A$ when data from the whole year were analyzed, because low photosynthetic rates outside of the growing season may cause high photosynthetic discrimination even when stomatal conductance is low (Table 4). McDowell *et al*. (2004a) found that *VPD* did not correlate with $\delta_R$ at the Metolius site in 2001, while Bowling *et al*. (2002) found such a correlation for several years across a precipitation gradient including the Metolius site. It is not clear why there was a difference in the correlation of $\delta_R$ with *VPD* between the two studies, but it could be accidental. *VPD* is not an independent driving factor of stomatal conductance and discrimination, but this value is related to temperature and humidity and can be correlated with radiation, which all effect simulated photosynthesis and stomatal conductance. The same values of *VPD* may result under different combinations of radiation, relative humidity and temperature, determining different $\delta_A$ for a given *VPD*, as shown in Figs. 7 and 8. This was also noted in the study of Baldocchi and Bowling (2003), who simulated isotope discrimination in a broad-leaved forest with the multilayer canopy model CANISOTOPE, using a similar canopy ecophysiology as in ISOLSM. They showed a negative relationship between photosynthetically active radiation and hourly discrimination during the growing season, but the discrimination values varied by up to 4–6‰ for a given value of photon flux density, reflecting the interactions of different factors (i.e. cloudiness and *VPD*) determining stomatal conductance, photosynthesis, and discrimination. Thus, different relations between *VPD* or other meteorological variables and observed discrimination can naturally occur across different sites and time periods, without indicating a difference in the controlling mechanisms of ecosystem discrimination.

The daily variability of $\delta_A$ simulated in this study is higher than the seasonal variability of $\delta_R$ observed in this (Fig. 6) and most other studies. We attribute this to the temporal lags of transport of assimilates to different respiratory plant parts that are not included in our model. These may be variable across sites and time periods (Bowling *et al*., 2002; McDowell *et al*., 2004a; Scartazza *et al*., 2004; Barbour *et al*., 2005; Knohl *et al*., 2005). These factors make it very difficult to relate $\delta_R$ data obtained at seasonal or monthly times scales to the instantaneous controlling environmental factors often used in correlation analysis. ISOLSM simulates the nonlinear effects of meteorology on physiological processes, and can allow us to better understand the isotopic patterns found in surveys of $\delta_R$ or other ecosystems components.

## Conclusions

This study shows that measurements of carbon isotope discrimination can be useful to constrain parameterizations of land surface models. A canopy scale model,

ISOLSM, driven by half-hourly meteorology was used to simulate carbon and energy fluxes and photosynthetic isotope discrimination. We compared observed and simulated *NEE*, *LE*, and *H* fluxes to estimate the parameters ($V_m$ and $m$, Eqns (1) and (6)) that provided the best fit to the data, but found that this approach resulted in a wide range of parameters that yielded similar fits (Table 3). The sensitivity of discrimination to the empirical parameter of the stomatal conductance equation, $m$, reduced the wide parameter space obtained from energy and carbon fluxes parameterizations (Table 3 and Fig. 1), providing an additional constraint to the model. We selected values of $m$ that resulted in a long-term integral of simulated discrimination similar to $\delta^{13}C$ values of sunlit old leaves of the same site. Foliar $\delta^{13}C$ values may represent a different time period than the model estimates, but better measurements of photosynthetic carbon isotope discrimination could improve the parameterization of land surface and carbon balance models.

We tested the model results against daily measurements of foliar and ecosystem respiration, and found that the variability of discrimination simulated with the selected parameters matched reasonably well the variability found in isotopic surveys of $\delta_R$ and $\delta_f$ (Fig. 6). Empirical relationships between discrimination, *VPD*, and other environmental factors observed in surveys of $\delta_R$ and $\delta_f$ were also found for simulated $\delta_R$ and $\delta_A$ (Fig. 8 and Table 4). The model tests showed that ISOLSM reasonably simulates the temporal variability of $\delta_A$ in response to atmospheric conditions, making it useful for the study of ecosystem carbon cycling processes and for the estimation of the temporal variability of $C_3$ terrestrial isotope discrimination.

## Acknowledgments

This manuscript is part of BASIN synthesis activities. We thank AmeriFlux and BASIN participants for making their Metolius data available, especially D. R. Bowling, who provided unpublished isotope data. We thank the comments of anonymous reviewers, which improved the manuscript. Support for BASIN and for J. Aranibar was provided by NSF. Support for J. Berry is provided by NASA (NAG5-9360), and for Law's Metolius AmeriFlux research by NASA (NAG5-7531) and the Department of Energy (DOE, FG0300ER63014).

## References

Anderson MC, Norman JM, Meyers TP *et al*. (2000) An analytical model for estimating canopy transpiration and carbon assimilation fluxes based on canopy light-use efficiency. *Agricultural and Forest Meteorology*, **101**, 265–289.

Anthoni PM, Law BE, Unsworth MH (1999) Carbon and water vapor exchange of an open-canopied ponderosa pine ecosystem. *Agricultural and Forest Meteorology*, **95**, 151–168.

Anthoni PM, Unsworth MH, Law BE *et al*. (2002) Seasonal differences in carbon and water vapor exchange in young and old-growth ponderosa pine ecosystems. *Agricultural and Forest Meteorology*, **111**, 203–222.

Baldocchi DD (1997) Measuring and modelling carbon dioxide and water vapour exchange over a temperate broad-leaved forest during the 1995 summer drought. *Plant, Cell and Environment*, **20**, 1108–1122.

Baldocchi DD, Bowling DR (2003) Modelling the discrimination of $^{13}CO_2$ above and within a temperate broad-leaved forest canopy on hourly to seasonal time scales. *Plant, Cell and Environment*, **26**, 231–244.

Baldocchi DD, Bowling DR (2005) Theoretical examination of keeling-plot relationships for carbon dioxide in a temperate broadleaved forest with a biophysical model, CANISOTOPE. In: *Stable Isotopes and Biosphere-Atmosphere Interactions: Processes and Biological Controls* (eds Flanagan LB, Ehleringer JR, Pataki DE, Mooney HA), pp. 109–124. Elsevier Press, San Diego, CA.

Baldocchi D, Falge E, Gu L *et al*. (2001) FLUXNET: a new tool to study the temporal and spatial variability of ecosystem-scale carbon dioxide, water vapor, and energy flux densities. *Bulletin of the American Meteorological Society*, **82**, 2415–2434.

Ball JT (1988) An analysis of stomatal conductance. PhD Thesis, Stanford University. Stanford, CA.

Barbour MM, Hunt JE, Dungan RJ *et al*. (2005) Variation in the degree of coupling between $\delta^{13}C$ of phloem sap and ecosystem respiration in two mature *Nothofagus* forests. *New Phytologist*, **166**, 497–512, doi:10.1111/j.1469-8137.2005.01329.x.

Bernacchi CJ, Singsaas EL, Pimentel C *et al*. (2001) Improved temperature response functions for models of Rubisco-limited photosynthesis. *Plant, Cell and Environment*, **24**, 253–259.

Bonan GB (1996) *A Land Surface Model (LSM version 1.0) for Ecological, Hydrological, and Atmospheric Studies: Technical Description and User's Guide*. National Center for Atmospheric Research, Boulder, CO.

Bowling DR, Cook CS, Ehleringer JR (2001a) Technique to measure $CO_2$ mixing ratio in small flasks with a bellows/IRGA system. *Agricultural and Forest Meteorology*, **109**, 61–65.

Bowling DR, McDowell NG, Bond BJ *et al*. (2002) C-13 content of ecosystem respiration is linked to precipitation and vapor pressure deficit. *Oecologia*, **131**, 113–124.

Bowling DR, McDowell NG, Welker JM *et al*. (2003) Oxygen isotope content of $CO_2$ in nocturnal ecosystem respiration: 1. Observations in forests along a precipitation transect in Oregon, USA. *Global Biogeochemical Cycles*, **17**, GB1120, doi:10.1029/2003GB002081.

Bowling DR, Tans PP, Monson RK (2001b) Partitioning net ecosystem carbon exchanges with isotopic fluxes of $CO_2$. *Global Change Biology*, **7**, 127–145.

Buchmann N, Kaplan JO (2001) Carbon isotope discrimination of terrestrial ecosystems- how well do observed and modeled results match? In: *Global Biogeochemical Cycles in the Climate System* (eds Schulze E-D, Heimann M, Harrison S, Holland E, Lloyd J, Prentice IC, Schimel DS), pp. 253–266. Academic Press Inc., San Diego.

Ciais P, Cuntz M, Scholze M *et al*. (2005) Remarks on the use of $^{13}C$ and $^{18}O$ isotopes in atmospheric $CO_2$ to quantify biospheric carbon fluxes. In: *Stable Isotopes and Biosphere–Atmo-*

*sphere Interactions: Processes and Biological Controls* (eds Flanagan LB, Ehleringer JR, Pataki DE, Mooney HA), pp. 235–267. Elsevier Press.

Ciais P, Tans PP, Trolier M *et al*. (1995) A large northern hemisphere terrestrial $CO_2$ sink indicated by the $^{13}C/^{12}C$ ratio of atmospheric $CO_2$. *Science*, **269**, 1098–1102.

Collatz GJ, Ball JT, Grivet C *et al*. (1991) Physiological and environmental regulation of stomatal conductance, photosynthesis, and transpiration: a model that includes a laminar boundary layer. *Agricultural and Forest Meteorology*, **54**, 107–136.

Collelo GD, Grivet C, Sellers PJ *et al*. (1998) Modeling of energy, water, and $CO_2$ flux in a temperate grassland ecosystem with SiB2: May–October 1987. *Journal of the Atmospheric Sciences*, **55**, 1141–1169.

Cooley HS, Riley WJ, Torn MS *et al*. (2005) Impact of agricultural practice on regional climate in a coupled land surface mesoscale model. *Journal of Geophysical Research*, **110**, doi:10.1029/2004JD005160.

Craig H (1954) Carbon 13 in plants and the relationships between carbon 13 and carbon 14 variations in nature. *The Journal of Geology*, **62**, 115–148.

Cuntz M, Ciais P, Hoffmann G *et al*. (2003) A comprehensive global three-dimensional model of delta super(18)O in atmospheric CO sub(2): 2. Mapping the atmospheric signal. *Journal of Geophysical Research. D. Atmospheres*, **108**, 4528, doi:10.1029/2002JD003154.

Dawson TE, Mambelli S, Plamboeck AH *et al*. (2002) Stable isotopes in plant ecology. *Annual Review of Ecology and Systematics*, **33**, 507–559.

Ehleringer JR, Cook CS (1998) Carbon and oxygen isotope ratios of ecosystem respiration along an Oregon conifer transect: preliminary observations based on small-flask sampling. *Tree Physiology*, **18**, 513–519.

Ekblad A, Högberg P (2001) Natural abundance of $^{13}C$ in $CO_2$ respired from forest soils reveals speed of link between tree photosynthesis and root respiration. *Oecologia*, **127**, 305–308.

Evans JR, Loreto F (2000) Acquisition and diffusion of $CO_2$ in higher plant leaves. In: *Photosynthesis: Physiology and Metabolism* (eds Leegood RC, Sharkey TD, von Caemmerer S), pp. 321–351. Kluwer Academic Press, The Netherlands.

Evans JR, von Caemmerer S (1996) Carbon dioxide diffusion inside leaves. *Plant Physiology*, **110**, 339–346.

Farquhar GD (1983) On the nature of carbon isotope discrimination in $C_4$ species. *Australian Journal of Plant Physiology*, **10**, 205–226.

Farquhar GD, Ehleringer JR, Hubick KT (1989) Carbon isotope discrimination and photosynthesis. *Annual Review of Plant Physiology and Plant Molecular Biology*, **40**, 503–537.

Farquhar GD, O'Leary MH, Berry JA (1982) On the relationship between carbon isotope discrimination and intercellular carbon dioxide concentration in leaves. *Australian Journal of Plant Physiology*, **9**, 121–137.

Farquhar GD, von Caemmerer S, Berry JA (1980) A biochemical model of photosynthetic $CO_2$ assimilation in leaves of $C_3$ species. *Planta*, **149**, 78–90.

Francey RJ, Allison CE, Welch ED (1995) The 11-year high precision in situ $CO_2$ stable isotope record from Cape Grim, 1982–1992. In: *Baseline Atmospheric Program (Australia) 1992* (eds Dick AL, Fraser PJ), pp. 16–25. Bureau of Meteorology and CSIRO Division of Atmospheric Research, Victoria, Australia.

Fung IY, Field CB, Berry JA *et al*. (1997) Carbon 13 exchanges between the atmosphere and biosphere. *Global Biogeochemical Cycles*, **11**, 507–533.

Ghashghaie J, Badeck FW, Lanigan G *et al*. (2003) Carbon isotope fractionation during dark respiration and photorespiration in $C_3$ plants. *Phytochemistry Reviews*, **2**, 145–161.

Ghashghaie J, Duranceau M, Badeck F-W *et al*. (2001) $\delta^{13}C$ of $CO_2$ respired in the dark in relation to $\delta^{13}C$ of leaf metabolites: comparison between *Nicotiana sylvestris* and *Helianthus annuus* under drought. *Plant, Cell and Environment*, **24**, 505–515.

Hammer C, Mayewski PA, Peel D *et al*. (1997) Greenland summit ice cores: Greenland Ice Sheet Project 2 (GISP2), and Greenland Ice Core Program (GRIP) Preface. *Journal of Geophysical Research*, **102**, 26315–26316.

Hemming DL, Yakir D, Ambus P *et al*. (2005) Pan-European $\delta^{13}C$ values of air and organic matter from forest ecosystems. *Global Change Biology*, **11**, doi:10.1111/j.1365-2486.2005.00971.x.

Hoefs J (1997) *Stable Isotope Geochemistry*. Springer, Berlin.

Hoffmann G, Cuntz M, Weber C *et al*. (2004) A model of the Earth's Dole effect. *Global Biogeochemical Cycles*, **18**, doi:10.1029/2003GB002059.

Högberg P, Nordgren A, Buchmann N *et al*. (2001) Large-scale forest girdling shows that current photosynthesis drives soil respiration. *Nature*, **411**, 789–792.

Indermühle A, Stocker TF, Joos F *et al*. (1999) Holocene carbon-cycle dynamics based on $CO_2$ trapped in ice at Taylor Dome, Antarctica. *Nature*, **398**, 121–126.

Irvine J, Law BE, Kurpius MR *et al*. (2004) Age related changes in ecosystem structure and function and the effects on water and carbon exchange in ponderosa pine. *Tree Physiology*, **24**, 753–763.

Irvine J, Law BE, Kurpius MR (2005) Coupling of canopy gas exchange with root and rhizosphere respiration in a semi-arid forest. *Biogeochemistry*, **73**, 271–282.

Kaplan JO, Prentice IC, Buchmann N (2002) The stable carbon isotope composition of the terrestrial biosphere: modeling at scales from the leaf to the globe. *Global Biogeochemical Cycles*, **16**, doi:10.1029/2001GB001403.

Keeling CD (1958) The concentration and isotopic abundances of atmospheric carbon dioxide in rural areas. *Geochimica et Cosmochimica Acta*, **13**, 322–334.

Keitel C, Adams MA, Holst T *et al*. (2003) Carbon and oxygen isotope composition of organic compounds in the phloem sap provides a short-term measure for stomatal conductance of European beech (*Fagus sylvatica* L.). *Plant, Cell and Environment*, **26**, 1157–1168.

Klumpp K, Schäufele R, Lötscher M *et al*. (2005) C-isotope composition of $CO_2$ respired by shoots and roots: fractionation during dark respiration? *Plant, Cell and Environment*, **28**, 241–250.

Knohl A, Werner RA, Brand WA *et al*. (2005) Short-term variations in $\delta^{13}C$ of ecosystem respiration reveals link between assimilation and respiration in a deciduous forest. *Oecologia*, **142**, 70–82.

Kurpius MR, Panek JA, Nikolov NT *et al*. (2003) Partitioning of water flux in a Sierra Nevada ponderosa pine plantation. *Agricultural and Forest Meteorology*, **117**, 173–192.

Lai C, Ehleringer JR, Tans PP *et al*. (2004) Estimating photosynthetic $^{13}C$ discrimination in terrestrial $CO_2$ exchange from canopy to regional scales. *Global Biogeochemical Cycles*, **18**, GB1041, doi:10.1029/2003GB002148.

Law BE, Cescatti A, Baldocchi DD (2001a) Leaf area distribution and radiative transfer in open-canopy forests: implications for mass and energy exchange. *Tree Physiology*, **21**, 777–787.

Law BE, Falge E, Baldocchi DD *et al*. (2002) Environmental controls over carbon dioxide and water vapor exchange of terrestrial vegetation. *Agricultural and Forest Meteorology*, **113**, 97–120.

Law BE, Sun OJ, Campbell J *et al*. (2003) Changes in carbon storage and fluxes in a chronosequence of ponderosa pine. *Global Change Biology*, **9**, 510–524.

Law BE, Thornton PE, Irvine J *et al*. (2001b) Carbon storage and fluxes in ponderosa pine forests at different developmental stages. *Global Change Biology*, **7**, 755–777.

Law BE, Williams M, Anthoni PM *et al*. (2000) Measuring and modelling seasonal variation of carbon dioxide and water vapour exchange of a *Pinus ponderosa* forest subject to soil water deficit. *Global Change Biology*, **6**, 613–630.

Leuning R, Dunin FX, Wang Y-P (1998) A two-leaf model for canopy conductance, photosynthesis and partitioning of available energy. Part II: comparison with measurements. *Agricultural and Forest Meteorology*, **91**, 113–125.

Lin GH, Ehleringer JR (1997) Carbon isotopic fractionation does not occur during dark respiration in $C_3$ and $C_4$ plants. *Plant Physiology*, **114**, 391–394.

Lloyd J, Farquhar GD (1994) $^{13}C$ discrimination during $CO_2$ assimilation by the terrestrial biosphere. *Oecologia*, **99**, 201–215.

McDowell NG, Bowling DR, Bond BJ *et al*. (2004a) Response of the carbon isotopic content of ecosystem, leaf, and soil respiration to meteorological and physiological driving factors in a Pinus ponderosa ecosystem. *Global Biogeochemical Cycles*, **18**, GB1013, doi:10.1029/2003GB002049.

McDowell NG, Bowling DR, Schauer A *et al*. (2004b) Associations between carbon isotope ratios of ecosystem respiration, water availability and canopy conductance. *Global Change Biology*, **10**, 1767–1784.

Miller JB, Tans PP, White JWC *et al*. (2003) The atmospheric signal of terrestrial carbon isotopic discrimination and its implications for partitioning carbon fluxes. *Tellus*, **55B**, 197–206.

Mortazavi B, Chanton JP, Prater JL *et al*. (2005) Temporal variability in $^{13}C$ of respired $CO_2$ in a pine and a hardwood forest subject to similar climatic conditions. *Oecologia*, **142**, 57–69.

Noone D, Still CJ, Riley WJ (2002) A global biophysical model of $^{18}O$ in terrestrial water and $CO_2$ fluxes. *World Meteorological Organization*, 32.

O'Leary MH (1984) Measurement of the isotope fractionation associated with diffusion of carbon dioxide in aqueous solution. *Journal of Physical Chemistry*, **88**, 823–825.

Ogee J, Peylin P, Ciais P *et al*. (2003) Partitioning net ecosystem carbon exchange into net assimilation and respiration using $^{13}CO_2$ measurements: a cost-effective sampling strategy. *Global Biogeochemical Cycles*, **17**, 1070, doi:10.1029/2002GB001995.

Ogee J, Peylin P, Cuntz M *et al*. (2004) Partitioning net ecosystem carbon exchange into net assimilation and respiration with canopy-scale isotopic measurements: an error propagation analysis with $^{13}CO_2$ and $CO^{18}O$ data. *Global Biogeochemical Cycles*, **18**, GB2019, doi:10.1029/2003GB002166.

Ometto JPH, Flanagan LB, Martinelli LA *et al*. (2002) Carbon isotope discrimination in forest and pasture ecosystems of the Amazon Basin, Brazil. *Global Biogeochemical Cycles*, **16**, 1109, doi:10.1029/2001GB001462.

Pataki DE, Ehleringer JR, Flanagan LB *et al*. (2003) The application and interpretation of Keeling plots in terrestrial carbon cycle research. *Global Biogeochemical Cycles*, **17**, GB1022, doi:10.1029/2001GB001850.

Pyles RD, Weare BC, Paw UKT (2000) The UCD advanced canopy-atmosphere-soil algorithm: comparisons with observations from different climate and vegetation regimes. *Quarterly Journal of the Royal Meteorological Society*, **126**, 2951–2980.

Randerson JT (2005) Terrestrial ecosystems and interannual variability in the global atmospheric budgets of $^{13}CO_2$ and $^{12}CO_2$. In: *Stable Isotopes and Biosphere–Atmosphere Interactions: Processes and Biological Controls* (eds Flanagan LB, Ehleringer JR, Pataki DE, Mooney HA), pp. 217–234. Elsevier Press, San Diego.

Randerson JT, Collatz GJ, Fessenden JE *et al*. (2002) A possible global covariance between terrestrial gross primary production and $^{13}C$ discrimination: consequences for the atmospheric $^{13}C$ budget and its response to ENSO. *Global Biogeochemical Cycles*, **16**, 1136, doi:10.1029/2001GB001845.

Riley WJ, Randerson JT, Foster PN *et al*. (2005) The influence of terrestrial ecosystems and topography on coastal $CO_2$ measurements: a case study at Trinidad Head, California. *Journal of Geophysical Research*, **110**, G01005, doi: 10.1029/2004JG000007.

Riley WJ, Still CJ, Helliker BR *et al*. (2003) Measured and modeled $^{18}O$ in $CO_2$ and $H_2O$ above a tallgrass prairie. *Global change Biology*, **9**, 1567–1581.

Riley WJ, Still CJ, Torn MS *et al*. (2002) A mechanistic model of $H_2$-$^{18}O$ and C-$^{18}OO$ fluxes between ecosystems and the atmosphere: model description and sensitivity analyses. *Global Biogeochemical Cycles*, **16**, 1095, doi:10.1029/2002GB001878.

Ropelewski CF, Halpert MS (1996) Quantifying Southern Oscillation–precipitation relationships. *Journal of Climate*, **9**, 1043–1059.

Scartazza A, Mata C, Matteaucci G *et al*. (2004) Comparisons of $\delta^{13}C$ of photosynthetic products and ecosystem respiratory $CO_2$ and their responses to seasonal climate variability. *Oecologia*, **140**, 340–351.

Scholze M, Kaplan JO, Knorr W *et al*. (2003) Climate and interannual variability of the atmosphere-biosphere $^{13}CO_2$ flux. *Geophysical Research Letters*, **30**, 1097, doi:10.1029/2002GL015631.

Schwarz PA, Law BE, Williams M *et al*. (2004) Climatic versus biotic constraints on carbon and water fluxes in seasonally drought-affected ponderosa pine ecosystems. *Global Biogeochemical Cycles*, **18**, GB4007, doi:10.1029/2004GB002234.

Sellers PJ, Randall DA, Collatz GJ *et al*. (1996) A revised land surface parameterization (SiB2) for atmospheric GCMs. Part I: model formulation. *Journal of Climate*, **9**, 676–705.

Still CJ, Berry JA, Collatz GJ *et al*. (2003) Global distribution of $C_3$ and $C_4$ vegetation: carbon cycle implications. *Global Biogeochemical Cycles*, **17**, 1006, doi:10.1029/2001GB001807.

Suits NS, Denning AS, Berry JA *et al*. (2005) Simulation of carbon isotope discrimination of the terrestrial biosphere. *Global Biogeochemical Cycles*, **19**, GB1017, doi:10.1029/2003GB002141.

Trolier M, White JWC, Tans PP *et al*. (1996) Monitoring the isotopic composition of atmospheric $CO_2$: measurements from the NOAA Global Air Sampling Network. *Journal of Geophysical Research*, **101**, 25897–25916.

Trudinger CM, Enting IG, Francey RJ *et al*. (1999) Long-term variability in the global carbon cycle inferred from a high-precision $CO_2$ and $\delta^{13}C$ ice-core record. *Tellus*, **51B**, 233–248.

Tu KP, Dawson TE (2005) Partitioning ecosystem respiration using stable carbon isotope analyses of $CO_2$. In: *Stable Isotopes and Biosphere–Atmosphere Interaction: Processes and Biological Controls* (eds Flanagan LB, Ehleringer JR, Pataki DE, Mooney HA), pp. 125–153. Elsevier Press, San Diego.

von Caemmerer S (2000) *Biochemical Models of Leaf Photosynthesis*. CSIRO, Australia.

von Caemmerer S, Evans JR, Hudson GS *et al*. (1994) The kinetics of ribulose-1,5-biphosphate carboxylase/oxygenase in vivo inferred from measurements of photosynthesis in leaves of transgenic tobacco. *Planta*, **195**, 88–97.

Williams M, Law BE, Anthoni PM *et al*. (2001) Use of a simulation model and ecosystem flux data to examine carbon-water interactions in ponderosa pine. *Tree Physiology*, **21**, 287–298.

Wilson KB, Baldocchi DD, Aubinet M *et al*. (2002) Energy partitioning between latent and sensible heat flux during the warm season at FLUXNET sites. *Water Resources Research*, **38**.